Molecular Batteries Based on Carbon–Carbon Bond Formation and Cleavage in Titanium and Vanadium Schiff Base Complexes

Federico Franceschi,[a] Euro Solari,[a] Carlo Floriani,*[a] Marzio Rosi,[b] Angiola Chiesi-Villa,[c] and Corrado Rizzoli[c]

Abstract: The reduction of titanium(III) and vanadium(III) salophen complexes led to the reductive coupling of imino groups in the ligands, and thus to the formation of C–C-bonded dimers which released electrons on subsequent cleavage of the C–C bond. On reduction of [M(salophen)(Cl)(thf)] [M = Ti (**1**), V (**2**)] with sodium metal in a 1:1 molar ratio the dimers [M_2(salophen$_2$)(thf)$_2$] [M = Ti (**3**), V (**4**)] formed, in which two salophen units are joined by a single C–C bond. Further reduction resulted in the introduction of an additional C–C bridge between the two salophen units and thus to the formation of [M_2(*salophen$_2$*)(Na)$_2$(thf)$_6$] [M = Ti (**6**), V (**7**)], in which *salophen$_2$* is a dinucleating, octadentate, octaanionic ligand. In **6** and **7**, the two metal centers are very close together [Ti···Ti = 2.518(1) Å in **6**; V···V = 2.393(1) Å in **7**]. Complexes **3** and **4** reacted with 9,10-phenanthrenequinone to give [M(salophen)(9,10-phen)] [M = Ti (**9**), V (**10**)], using both the electrons stored at the C–C bond and those from the oxidation of M^{III} to M^{IV}. The reaction of **3** and **4** with O_2 yielded the oxometal(IV) complexes [M(salophen)(O)] [M = Ti (**13**), V (**11**)] with a four-electron oxidation of the starting dimers. The intermediate oxovanadium(III) complex [V(salophen){μ-O-Na(DME)$_2$}] (**16**), which can be subsequently oxidized to **11**, was isolated from the reaction of **7** with O_2. The reaction became synthetically and mechanistically interesting when organic azides were used as oxidizing agents: reaction of **3** with PhN_3 and Me_3SiN_3 led to the μ-phenylimido dimers [Ti_2(salophen$_2$)(μ-PhN)(thf)$_2$] (**17**) and [Ti_2(salophen$_2$)(μ-Me_3SiN)] (**18**), which was hydrolyzed to the analogous μ-oxo [{Ti_2(salophen$_2$)(μ-O)}$_2$] (**19**). The reaction of **3** with Ph_3CN_3 led to the phenylimido complex [Ti(salophen)(NCPh$_3$)] (**20**), and **4** reacted with PhN_3 to give [V(salophen)(NPh)] (**21**). Extended Hückel calculations enabled us to substantiate the electron-transfer process, which never involves the C–C site as a reactive center; it only functions as an electron reservoir.

Keywords: electron transfer · molecular devices · redox chemistry · Schiff bases · titanium · vanadium

Introduction

The redox chemistry of transition metal complexes containing either macrocyclic or polydentate ligands essentially involves variations in the oxidation state of the metal centers. The metal-assisted redox chemistry of the macrocyclic or polydentate ligand has been studied far less, coming into play only when the delocalization of electrons or positive charges over a π-delocalized system is concerned.[1] Very rarely does the redox chemistry of the ligand have chemical consequences, such as the formation or cleavage of bonds, and even more rarely is this event reversible. A successful approach to this field would provide the possibility of storing and releasing electrons, a process which could be coupled to the variation in the oxidation state of the metal and which would produce a type of molecular battery.[2]

We approached this goal by studying the redox chemistry of transition metals bonded to tetradentate, highly π-delocalized Schiff bases, and choose titanium(III) and vanadium(III) bound to the salophen [*N*,*N*′-phenylenebis(salicylideneiminato) dianion] ligand as model compounds. In such a chemical environment, it is difficult to reduce titanium and vanadium to lower oxidation states; thus the reduction affected the ligand exclusively. This investigation led us to discover the reductive coupling of imino groups across two monomeric units, with the consequent formation of C–C bonds which function as reversible reservoirs of two electrons. They can be coupled or not with the metal, to function as long-range electron-transfer agents. Some results in this field, with

[a] Prof. Dr. C. Floriani, Dr. E. Solari, F. Franceschi
Institut de Chimie Minérale et Analytique, Université de Lausanne
BCH, CH-1015 Lausanne (Switzerland)
Fax: (+41) 21-6923905
E-mail: carlo.floriani@icma.unil.ch

[b] Dr. Marzio Rosi
Dipartimento di Chimica, Università di Perugia (Italy)

[c] Prof. Dr. A. Chiesi-Villa, Dr. C. Rizzoli
Dipartimento di Chimica, Università di Parma (Italy)

0947-6539/99/0502-0708 $ 17.50+.50/0 *Chem. Eur. J.* **1999**, *5*, No. 2

transition metals such as zirconium,[3] cobalt,[4] nickel,[5] and manganese,[2] have already been reported, while the structure of one of the vanadium complexes has been communicated.[6] We report herein the synthesis, structure, and chemical behavior of titanium(III) and vanadium(III) salophen complexes reductively coupled to dimers and bridged by one or two single C–C bonds. In contrast to work previously reported[2–6] in this field, we were able to explore the reactivity of the reduced species of the titanium and vanadium compounds described here. In these reactions the electrons stored at the C–C bond and in the metal atom can be selectively used, either separately or all together, in the reduction of O_2, quinones, and other substrates. An extended Hückel analysis substantiated the hypothesis that the reduction of Ti^{III} and V^{III} salophen complexes occurs with the electron density stored at the carbon centers involved in the C–C bridges across the two salophen units. The same calculations suggest that the first step in the transfer of the electrons stored at the C–C bonds occurs with the oxidation of the metal, followed by an electron withdrawal from nitrogen, and finally with the cleavage of the C–C bridge, which is never involved directly as a reactive site.

Results and Discussion

Reductive coupling to produce C–C bonds across two metal–salophen units: The synthesis of the starting titanium(III)[7] and vanadium(III)[8] Schiff base complexes was performed as reported in Scheme 1, by reaction of the sodium salt of the Schiff base, prepared in situ, with the corresponding metal(III) chloride. In the case of vanadium, there is an alternative synthesis starting from the free Schiff base and $VCl_3 \cdot 3\,thf$ in the presence of tBu_3N (see Method B in the Experimental Section). Complexes **1** and **2** have been fully characterized (see Experimental Section), including an X-ray analysis of **2**,[8] which demonstrates the hexacoordination of the metal and the planar arrangement of the salophen ligand.

Complexes **1** and **2** undergo stepwise reduction with sodium metal in THF to **6** and **7**, respectively. The sequence is shown in Scheme 2, whose upper part presents the structural consequences on the two salophen skeletons upon reduction,

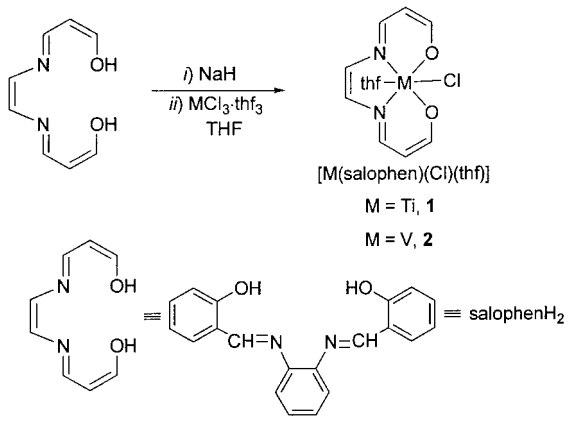

Scheme 1. Synthesis of the starting compounds.

while the lower part consists of the corresponding chemical equations. The starting materials **1** and **2** are drawn as two overlapping, nonbonded, monomeric, cationic units. We have omitted the THF and Cl^- in the coordination sphere of the metal. The one-electron reduction of **1** and **2** does not change the oxidation state (+3) of the metal. The chloride anion is removed as NaCl, and one electron is introduced into each monomer, resulting in a reductive coupling between two imino groups and the formation of C–C bonded dimer.

Recrystallization of **4** in the presence of pyridine gave crystals of $[V_2(salophen_2)(Py_2)]$ (**5**) that were suitable for X-ray analysis. The structural analysis of **5** (vide infra) shows, however, that the C–C bond formation is accompanied by the sharing of one of the oxygens of the Schiff base across the two vanadium ions. The introduction of two further electrons into the dimers **3** and **4** probably generates a diradical at the imino groups and leads to a second C–C coupling. Such a coupling is accompanied by a change in the bonding mode of the salophen skeleton, which can be visualized by rotating all the oxygen arms in opposite directions, as can be followed with the oxygen labeling employed in Scheme 2. At the same time, each nitrogen atom bridges the two metal atoms. The oxygen labeling in Scheme 2 shows that the two-electron reduction of **1** and **2** not only results in the formation of a C–C bond, but also causes the exchange of the two salophen skeletons between the two metal centers. The degree of

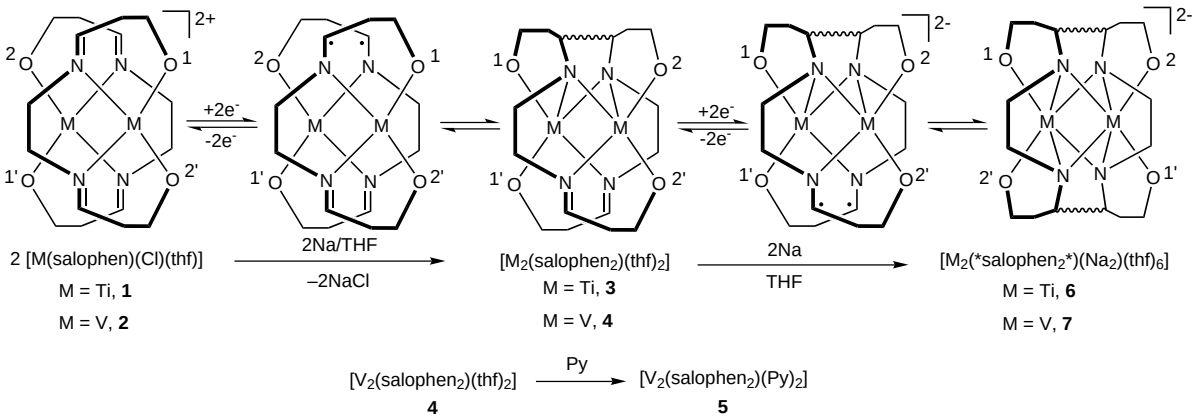

Scheme 2. The redox pathway showing the reversible formation and cleavage of C–C bonds. In the structural representation, THF and Cl^- in the coordination sphere of the metal have been omitted for the sake of clarity.

  0947-6539/99/0502-0709 $ 17.50+.50/0

coupling, that is the formation of one or of two C–C bonds, between the two starting monomeric units is controlled by the molar ratio between the metal and the reducing agent, which is exactly 1:1 for **3** and **4** and 1:2 for **6** and **7**. The second step in the reduction process proceeds either intramolecularly, as reported here for titanium and vanadium, or intermolecularly, as in the case of nickel, which yields a C–C-bridged polymer.[5] The choice between the two pathways is controlled by the coordination sphere of the metal, which is pentacoordinate or hexacoordinate in the case of Ti, V, and Mn,[2] unlike Ni^{II},[5] which remains strictly planar tetracoordinate in such an environment.

Complexes **3**–**7** have been fully characterized; X-ray structural analyses for **5**–**7** have been carried out. Crystal data are given in Table 1 and selected bond lengths and angles in Table 2. The structure of **5** displays the main features given in Scheme 2. Crystals suitable for X-ray analysis were obtained from pyridine, which replaces thf in the coordination sphere of the metal. The dimer shown in Figure 1 has a crystallographically imposed C_2 symmetry, with the twofold axis running perpendicular to the C(7)–C(7′) bond (1.595(5) Å, Table 2). Vanadium has a distorted octahedral coordination with the equatorial plane defined by the N_2O_2 set of donor atoms from salophen, and the axial positions filled by pyridine and the oxygen O(1′) of the adjacent salophen. The N_2O_2 core is planar, the deviations from planarity ranging from −0.009(3) to 0.009(3) Å for N(1) and N(2), respectively. As a consequence of the C–C bond formation, the six-membered chelating ring involving C(7) is folded along the C(7)···O(1) line; the dihedral angle between the V(1)-N(1)-C(7)-O(1) and the O(1)-C(1)-C(6)-C(7) mean planes is 40.7(2)°. The V–O and V–N distances are close to those found in **2**,[8] while the distances of vanadium to the bridging oxygens are much longer [V(1′)–O(1) 2.052(3); V(1)–O(1′) 2.055 Å]. The original salophen ligand has been converted in the reduction, assisted by the metal, into the dinucleating hexaanionic $salophen_2$, which holds the two metal ions rather close [V(1)···V(1′) 3.099 Å].

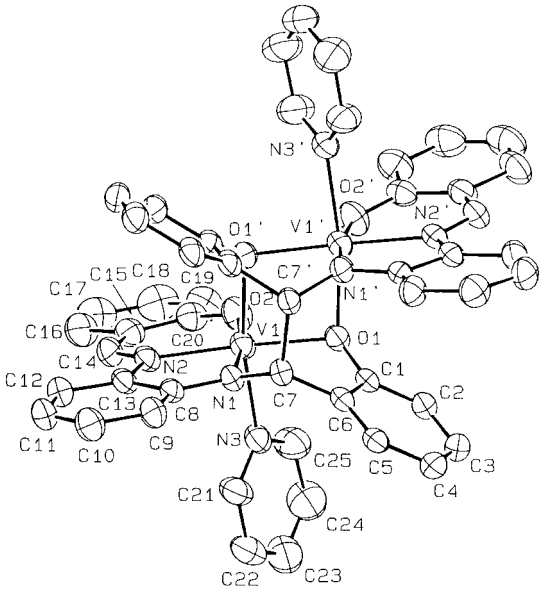

Figure 1. ORTEP view of complex **5** (30% probability ellipsoids). The prime denotes a transformation of $-x, y, 0.5-z$.

The major structural changes between **3**/**4** and **6** (Figure 2)/**7** (Figure 3) are depicted in Scheme 2.

The salophen moieties coupled by two C–C bonds [C(7)–C(14)′, 1.605(6) Å in **6** and 1.585(6) Å in **7**] form the centrosymmetric, dinucleating, octaanionic *$salophen_2$* ligand, which has been drawn without the metal centers in Figure 4. The two centrosymmetric metal atoms are bonded to the opposite sides of the centrosymmetric N(4) planar core at distances ranging from 2.120(4) to 2.135(2) Å in **6** and from 2.054(2) to 2.072(3) Å in **7**. The coordination around each metal is completed by two *cis*-arranged oxygens [O(1), O(2) around Ti(1) or V(1)] (Figure 5). Referring to Figure 5, it should be mentioned that i) the metal ion does not occupy the center of the prism; the displacements from the three faces O(1),O(2),N(1),N(2), O(1),O(2),N(1)′,N(2)′, and

Table 1. Crystallographic data for complexes **5**–**7**, **16**, **19**, and **20**.

Complex	**5**	**6**	**7**	**16**	**19**	**20**
formula	$C_{50}H_{38}N_6O_4V_2\cdot 3C_4H_8O$	$C_{68}H_{84}N_4Na_2O_{11}Ti_2\cdot 2C_4H_8O$	$C_{64}H_{76}N_4Na_2O_{10}V_2\cdot 2C_4H_8O$	$C_{48}H_{48}N_4Na_2O_{10}V_2$	$C_{80}H_{56}N_8O_{10}Ti_4\cdot 2C_7H_8$	$C_{39}H_{29}N_3O_2Ti$
a [Å]	15.742(1)	12.971(5)	21.275(2)	12.026(2)	12.502(2)	9.528(1)
b [Å]	20.343(2)	13.806(5)	17.029(2)	20.888(3)	14.800(3)	17.573(3)
c [Å]	17.262(2)	12.527(5)	19.552(2)	9.641(1)	11.190(2)	18.534(3)
α [°]	90	95.87(3)	90	92.56(2)	97.72(2)	90
β [°]	94.30(1)	115.91(2)	100.90(1)	106.98(2)	108.16(2)	90
γ [°]	90	62.26(3)	90	92.71(2)	79.19(1)	90
V [Å^3]	5512.4(9)	1771.4(14)	6955.7(13)	2309.3(6)	1926.0(7)	3103.3(8)
Z	4	1	4	1	2	1
M_r	1105.1	1419.4	1353.4	988.8	1665.3	619.6
space group	*C2/c* (No. 15)	$P\bar{1}$ (No. 2)	*C2/c* (No. 15)	$P\bar{1}$ (No. 2)	$P\bar{1}$ (No. 2)	$P2_12_12_1$ (No. 19)
T [°C]	22	−135	22	−135	−135	22
λ [Å]	0.71069	1.5478	0.71069	1.54178	1.54178	0.71069
ρ_{calcd} [g cm^{-3}]	1.332	1.331	1.292	1.422	1.436	1.326
μ [cm^{-1}]	3.84	25.66	3.31	41.26	39.78	3.09
transm. coeff.	0.907–1.000	0.766–1.000	0.968–1.000	0.725–1.000	0.744–1.000	0.929–1.000
R[a]	0.052	0.070	0.053	0.054	0.055	0.060 [0.064]
$wR2$[b]	0.122	0.208	0.136	0.161	0.163	0.120 [0.127]

[a] $R=\Sigma\,|\Delta F|/\Sigma\,|F_o|$ based on the unique observed data [$I>2\sigma(I)$]. [b] $wR2=[\Sigma w\,|\Delta F^2|^2/\Sigma w\,|F_o^2|^2]^{1/2}$ calculated on the unique data with $I>0$.

0947-6539/99/0502-0710 $ 17.50+.50/0 *Chem. Eur. J.* **1999**, *5*, No. 2

Table 2. Selected bond lengths [Å]and angles [°] for complexes **5**–**7**, **16**, **19**, and **20**.

5[a]		**6**[b]		**7**[c]		**16**[d]		**19**[e] Molecule A		**19**[e] Molecule B	**20**	
V(1)–O(1)	2.052(3)	Ti(1)–O(1)	2.050(3)	V(1)–O(1)	1.999(2)	V(1)–O(1)	1.954(3)	Ti(1)–O(1)	1.832(5)	1.823(5)	Ti(1)–O(1)	1.915(4)
V(1)–O(1)′	2.055(4)	Ti(1)–O(2)	2.052(3)	V(1)–O(2)	1.993(2)	V(1)–O(2)	1.930(4)	Ti(1)–O(2)	1.883(6)	2.035(5)	Ti(1)–O(2)	1.902(4)
V(1)–O(2)	1.925(2)	Ti(1)–O(5)	2.363(3)	V(1)–N(1)	2.054(3)	V(1)–O(3)	1.617(4)	Ti(1)–O(3)	1.787(4)	1.847(5)	Ti(1)–N(1)	2.153(4)
V(1)–N(1)	1.955(4)	Ti(1)–N(1)	2.135(3)	V(1)–N(1)′	2.065(2)	V(1)–N(1)	2.036(4)	Ti(1)B–O(2)B′		2.144(5)	Ti(1)–N(2)	2.151(4)
V(1)–N(2)	2.064(3)	Ti(1)–N(2)	2.132(4)	V(1)–N(2)	2.054(2)	V(1)–N(2)	1.994(4)	Ti(1)–N(1)	1.996(7)	1.987(4)	Ti(1)–N(3)	1.686(4)
V(1)–N(3)	2.170(4)	Ti(1)–N(1)′	2.127(3)	V(1)–N(2)′	2.072(3)	N(1)–C(7)	1.350(7)	Ti(1)–N(2)	2.147(6)	2.153(6)	N(1)–C(7)	1.293(9)
N(1)–C(7)	1.465(5)	Ti(1)–N(2)′	2.120(4)	N(1)–C(7)	1.470(5)	N(2)–C(14)	1.400(8)	N(1)–C(7)	1.464(9)	1.484(8)	N(2)–C(14)	1.295(7)
N(2)–C(14)	1.293(7)	N(1)–C(7)	1.458(7)	N(1)–C(8)	1.409(4)	Na(1)–O(1)	2.309(4)	N(2)–C(14)	1.315(11)	1.278(12)	N(3)–C(21)	1.469(6)
C(7)–C(7)′	1.595(5)	N(1)–C(8)	1.400(6)	N(2)–C(13)	1.407(5)	Na(1)–O(2)	2.289(4)	C(7)A–C(7)B	1.587(10)		Ti(1)-N(3)-C(21)	174.1(3)
		N(2)–C(13)	1.395(5)	N(2)–C(14)	1.462(5)	Na(1′)–O(3)	2.284(4)					
		N(2)–C(14)	1.470(6)	C(7)–C(14)′	1.585(6)							
		C(7)–C(14)′	1.605(6)									

[a] ′ = $-x$, y, $0.5-z$. [b] ′ = $-x$, $1-y$, $-z$. [c] ′ = $0.5-x$, $0.5-y$, $-z$. [d] ′ = $-1-x$, $-y$, $1-z$. [e] ′ = $-x$, $1-y$, $1-z$.

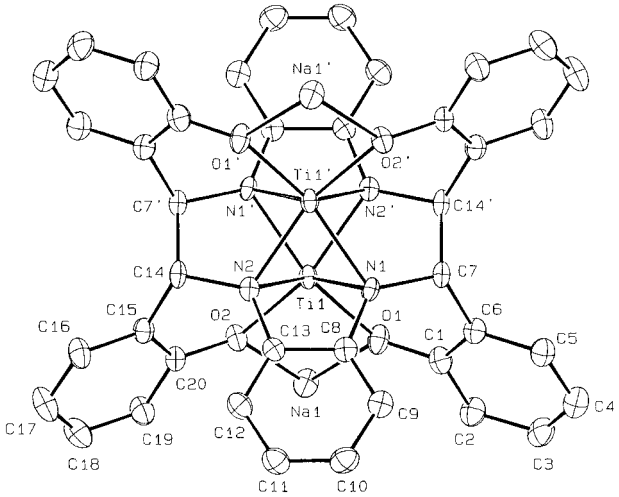

Figure 2. ORTEP view of complex **6** (50% probability ellipsoids). THF molecules are omitted for clarity. The prime denotes a transformation of $-x$, $1-y$, $-z$.

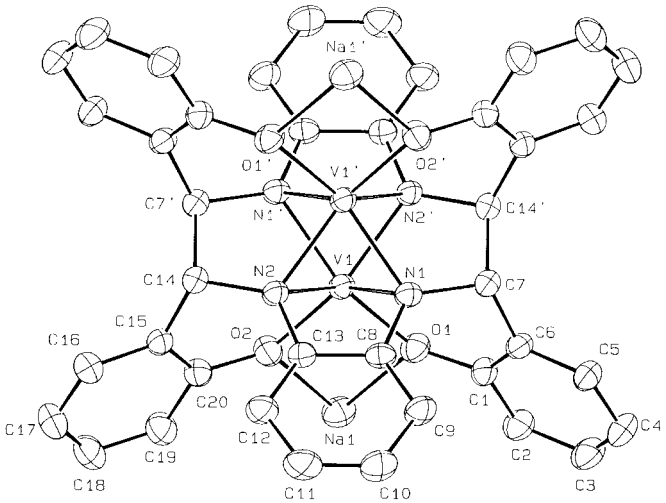

Figure 3. ORTEP view of complex **7** (30% probability ellipsoids). THF molecules are omitted for clarity. The prime denotes a transformation of $0.5-x$, $0.5-y$, $-z$.

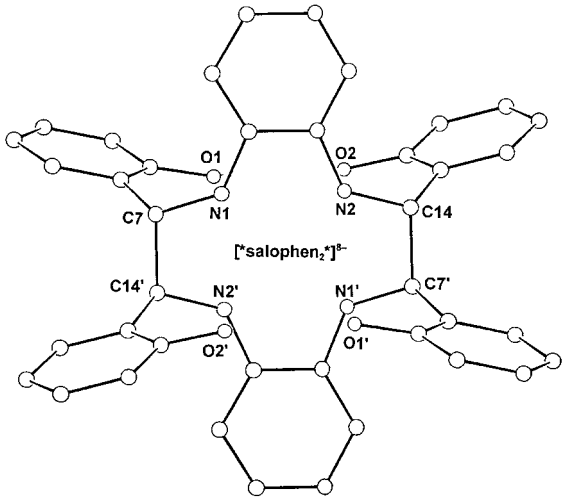

Figure 4. Numbering scheme of the *salophen$_2$* ligand.

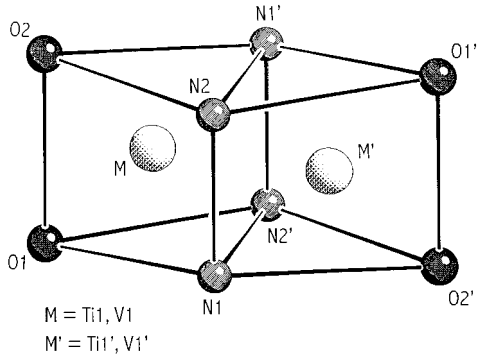

Figure 5. SCHAKAL drawing of the coordination polyhedra around titanium and vanadium cations in complexes **6** and **7**, respectively.

N(1),N(2),N(1)′,N(2)′ are 0.825(2), 0.364(1), and 1.259(1) for **6**, and 0.706(1), 0.495(1), and 1.196(1) Å for **7**, respectively; ii) the Ti(1)–Ti(1)′ separation is 2.518(1) and V(1)–V(1)′ is 2.393(1) Å. Such a short metal–metal distance is particularly relevant in the explanation of the magnetic properties of **6** and **7**. The *salophen$_2$* ligand defines an approximately planar 12-membered ring (see Figure 4) (maximum deviation 0.090(4) Å for N(1) in **6** and 0.103(4) Å for C(7)) which is

almost coplanar with the two *o*-phenylenediamine rings C(8)···C(13); the dihedral angle is 6.5(1)° in **6** and 2.4(1)° in **7**. A better description of the macroring is that formed by two nearly planar N(1),N(2),C(7),C(8),C(13),C(14) and N(1)′,N(2)′,C(7)′,C(8)′,C(13)′,C(14)′ moieties [maximum displacement 0.079(4) Å for C(14) in **6**, and 0.085(4) for C(7) in **7**] which are parallel from symmetry requirements and separated by 0.153(8) in **6**, and 0.065(7) Å in **7**. The N_2O_2 cores are almost perpendicular to the planar macroring system [dihedral angle 88.0(1)° in **6** and 73.1(1)° in **7**] and to the C(8)···C(13) aromatic ring [dihedral angle 84.3(1)° in **6** and 75.5(1)° in **7**]. The Ti–O, Ti–N, V–O, and V–N bond lengths (Table 2) are close to those of titanium(III) and vanadium(III) bonded to the Schiff base ligands previously reported. The conformation of the ligands gives rise to cavities which can accommodate two centrosymmetric sodium cations; each cation is bonded to the O(1) and O(2) oxygen atoms of the same Schiff base (Figures S1 and S2 in the information deposited at FIZ). Coordination around Na(1) is completed by the O(3), O(4), O(5) oxygen atoms from three THF molecules to give a distorted square pyramid. A further THF molecule was found to be disordered about the inversion center at $1-x, -y, 1-z$ in such a way as to provide a partial sixth coordination site to two sodium cations which belong to adjacent dimeric units, and which are symmetry-related by the inversion center, in the case of **6**.

At this stage we should comment on an important structural parameter in **6** and **7**, namely the very short metal–metal bond length. The metal–metal separation, per se, seems to suggest a direct metal–metal interaction,[9] though we are aware that such a geometric proximity may be the consequence of the constraint imposed by the very crowded dinucleating *salophen$_2$* ligand. We expected that some evidence for the existence of a metal–metal interaction would come from the analysis of the magnetic properties of **6** and **7** (Figure 6). The temperature dependence of the magnetic moments of **3** and **4** are typical of antiferromagnetically coupled Ti^{III} and V^{III} dimers, respectively. Effective magnetic moments close to the expected values of 1.73 and 2.83 BM are observed at room temperature with a strong decrease as the temperature is lowered. Essentially diamagnetic behavior is shown by **6** and **7**, although the latter compound shows a residual paramagnetism with a value of almost 1 BM at room temperature. Such behavior can be attributed to a high temperature-independent paramagnetism (TIP), probably as a result of the presence of a low-lying, thermally nonpopulated, paramagnetic excited state.[10] Therefore, we remain with the hypothesis of a considerable degree of metal–metal single bond character in **6**, and a double bond in **7**.

The alternative synthesis of **3** and **4** led us to discover a major property of the C–C bound Schiff base ligands: mixing equimolar amounts of **1** and **6** or **2** and **7** in THF at room temperature led to high yields of **3** and **4** as red-brown crystals (Scheme 3), through the same steps depicted in detail in Scheme 2. The occurrence of such a reaction is significant in many respects: i) the C–C bond formation and cleavage is reversible (see the reduction of **3** and **4** to **6** and **7**, and reaction in Scheme 3); ii) the C–C bond functions as a shuttle for two

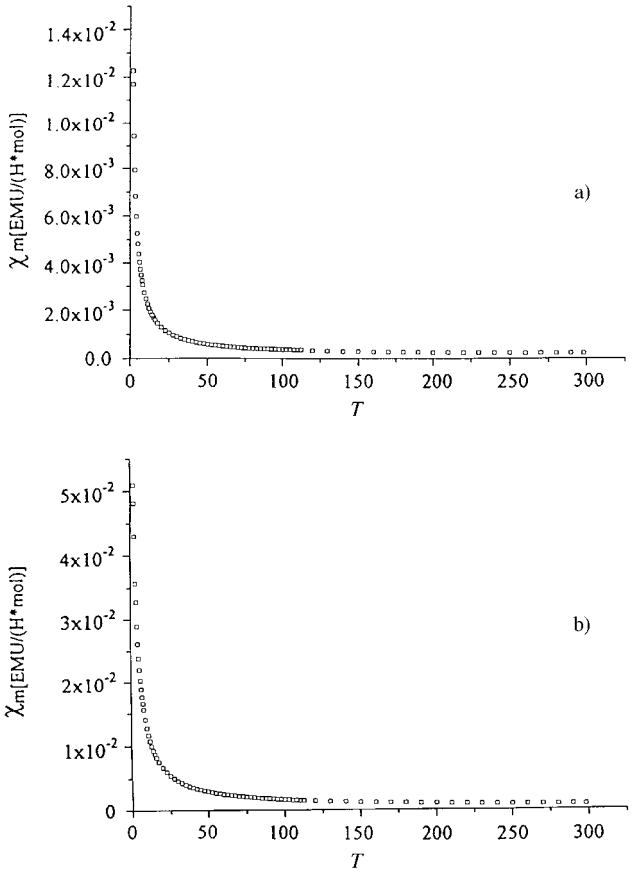

Figure 6. Magnetic properties of a) **6** and b) **7**.

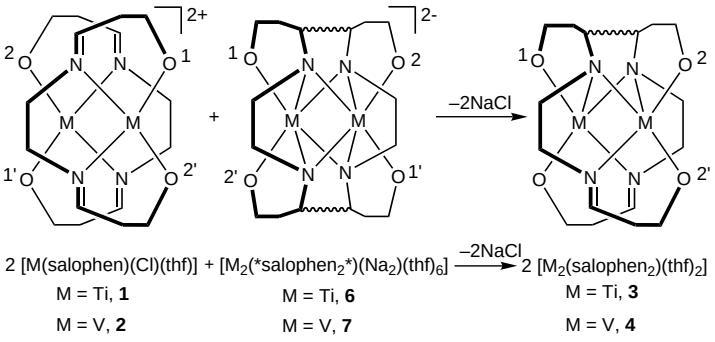

Scheme 3. The intermolecular electron transfer which occurs with cleavage and formation of the C–C bond.

electrons; iii) such an electron transfer can occur intermolecularly. As far as the last point is concerned, we believe that the reaction within the two complexes **1** and **6** or **2** and **7** is most probably assisted by the alkali cations, which allow the two species to come in contact by coordination to the same sodium ions.[11]

The C–C bond functioning as a two-electron reservoir: The most attractive property of complexes **3**–**7** is their tendency to function as reducing agents. Depending on the oxidation agent, both the electron stored at the C–C bond and/or the electrons available from the low oxidation state of the metal can be made accessible. In Scheme 4 we report reactions in which only the electrons stored at the C–C bond are used. In

0947-6539/99/0502-0712 $ 17.50+.50/0 *Chem. Eur. J.* **1999**, *5*, No. 2

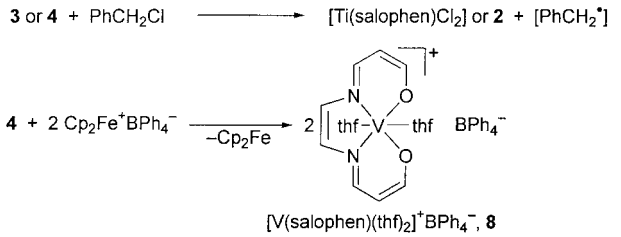

Scheme 4. The C–C bond functioning as an electron reservoir.

the reaction of **3** and **4** with benzyl chloride we observed the formation of [Ti(salophen)Cl_2] and **2** respectively, along with toluene as a result of hydrogen abstraction from the solvent, and 1,2-diphenylethane from the dimerization of the benzyl radical. The reaction of **4** with $[Cp_2Fe]^+[BPh_4]^-$ implies electron transfer only, without the formation of any chemical bond with the oxidized substrate in **8**.[12] The preferential use of **3** and **4** rather than **6** and **7** as electron transfer agents is due to their neutral form, since the identification of the reaction products in the latter case requires the separation of the titanium and vanadium derivatives from the sodium salts derived from the reduction of the substrate.

In this context we examined the reaction of **3**–**7** with dioxygen and *o*- and *p*-quinones, which can be considered as electronically equivalent. Quinones function primarily as two- rather than four-electron oxidizing agents, and the reduced form remains bonded to the metal without providing any oxo species. In the reaction shown in Scheme 5, *o*-phenanthrenequinone was treated with **3** and **4** in THF solution. On

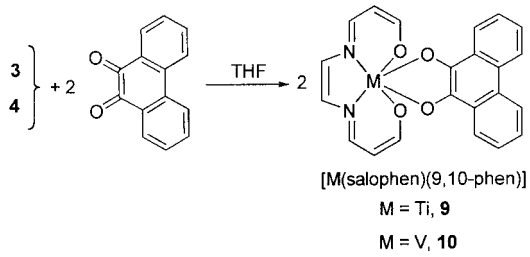

Scheme 5. The two-electron transfer from the C–C bond to 9,10-phenanthrenequinone.

refluxing the suspension we obtained the brown-red microcrystalline solids **9** and **10**. They have been fully characterized, including a preliminary X-ray analysis of **9** recrystallized from DMSO. Although the atom connectivity is quite well defined, the crystallographic structural data are so far very poor. The reaction in Scheme 5 is a two-electron oxidation per monomeric fragment; one electron comes from the C–C bond and the other from the oxidation of M^{III} to M^{IV}. In fact, **9** is a diamagnetic titanium(IV) derivative, for which the ^{1}H NMR spectrum has been recorded (see the Experimental Section), and **10** is a vanadium(IV) derivative [$\mu_{eff} = 1.61$ BM at 293 K]. The two-electron reduced form of 9,10-phenanthrenequinone mimics the *cis* bonding mode of the peroxo species. The reaction of **4** with *p*-benzoquinone (Scheme 6), which should mimic dioxygen to give the *trans*-peroxo-type of species, led, unexpectedly, to its unprecedented deoxygenation and thus to the formation of the oxovanadium(IV) derivative **11**. In the

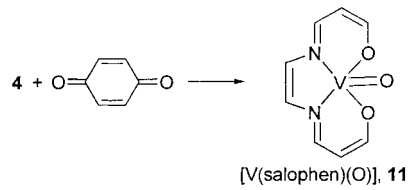

Scheme 6. The deoxygenation of *p*-benzoquinone.

reactions represented in Schemes 5 and 6 we observed a four-electron oxidation of the dimer; two electrons were supplied by the cleavage of the C–C bond and two by the oxidation of the two metal atoms ($M^{III} \rightarrow M^{IV}$). The reactions of **3** and **4** with dioxygen (Scheme 7) emphasizes the major differences between titanium and vanadium as a result of the difference in the relative stability of the corresponding monomeric metal(IV)oxo derivatives.[13]

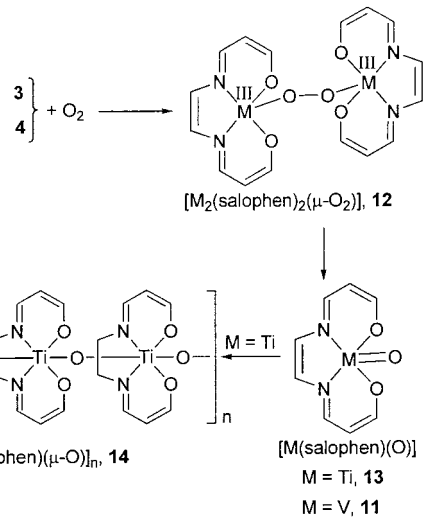

Scheme 7. The electron transfer from C–C bonds to dioxygen, mediated by titanium and vanadium.

Both compounds absorb dioxygen in an O_2/dimer molar ratio of 1:1. The plausible peroxo species **12** undergoes a different evolution, depending on the nature of the metal, to give a stable monomeric oxometal(IV), **11** in the case of vanadium, while in the case of titanium the derivative **13** polymerizes,[14] usually to **14**. It has to be mentioned that the terminal oxotitanium(IV) moiety has only rarely been identified and structurally characterized.[14–16] In order to show that **6** and **7**, which contain two C–C bonds, can be involved equally well in redox processes, we treated **7** with dioxygen (Scheme 8). The reaction proceeds with the very rapid absorption of a mole of O_2, followed by slower absorption of a second mole per mole of starting material. The reaction terminates with the formation of [VO(salophen)] (**11**) and sodium peroxide. A plausible pathway can be drawn, based on the isolation of the intermediate **16**, which is intercepted when the reaction is carried out with a limited amount of oxygen. The first compound to form is probably the μ-peroxo species **15**, which still contains a C–C bond across the two Schiff base units; this is presumably followed by the simultaneous cleavage of the O–O and the C–C bonds. The reaction leads

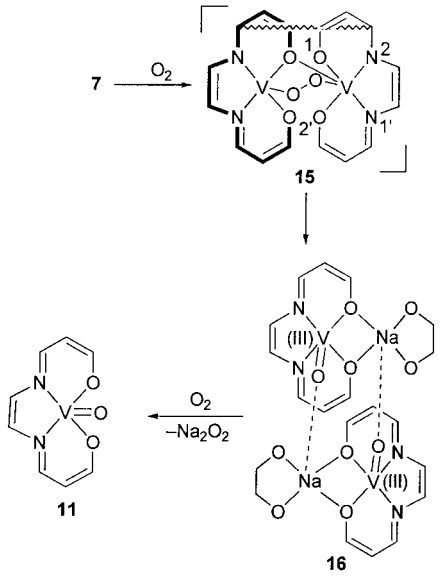

Scheme 8. Reduction of dioxygen with electrons stored in the vanadium molecular battery.

to the formation of a quite unusual oxovanadium(III) complex dimer,[17] **16**, which can, eventually, absorb a further mole of dioxygen to give the oxovanadium(IV) complex **11** and sodium peroxide. The low yield of **16** is a consequence of the sensitivity of **16** to oxygen.

Complex **16** consists of two crystallographically independent $[VO(salophen)]^-$ anions, bridged in centrosymmetric dimers by two $[Na(DME)]^+$ cations (Figure 7). Since the crystals contain two independent dimers, the structural

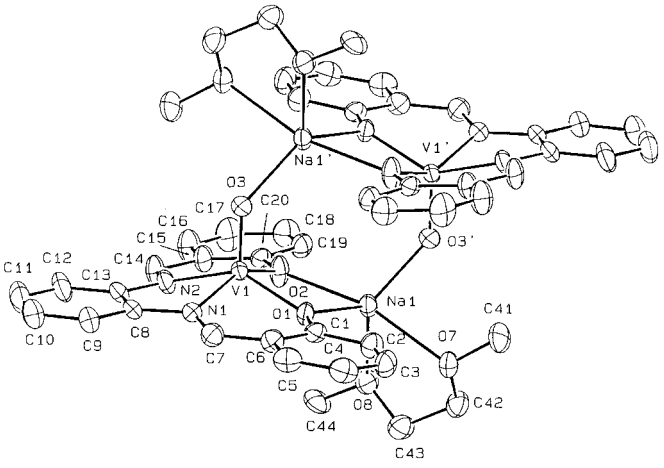

Figure 7. ORTEP view of molecule 1 in complex **16** (50% probability ellipsoids). The prime denotes a transformation of $-1-x, -y, 1-z$.

parameters will be discussed only for the dimer containing V(1). Vanadium has a square-pyramidal coordination, in which the N_2O_2 set of atoms from the salophen ligand defines the base and the O(3) oxo oxygen atom is at the apex. The metal is displaced from the mean basal plane by 2.205(4) Å, with a V–O distance of 1.617(4) Å. As is usual in pentacoordinated salophen–metal complexes, the ligand assumes a nearly planar conformation. Coordination around the sodium cation is provided by the O(1) and O(2) atoms from the Schiff base and by the O(3)′ oxo atom from the vanadyl fragment, which are symmetry-related by the inversion center. Two oxygen atoms from a DME molecule complete the coordination to produce a distorted trigonal bipyramid.

The reaction of **3** and **4** with organic azides, which are the source of the nitrene PhN, which is electronically equivalent to O, parallels the reaction with oxo-transfer reagents.[13] Such a reaction is not only mechanistically interesting with regard to our work, but it is also a novel synthetic approach to terminal and bridging metal–amido derivatives.[13]

The results from the reaction of **3** with organic azides are summarized in Scheme 9. A significant dependence on the R substituent and the metal has been observed. The reaction of **3**

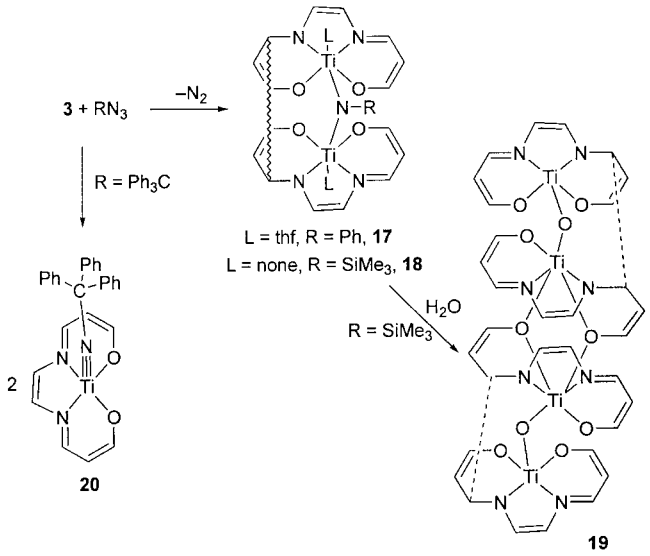

Scheme 9. Formation of imido complexes of titanium with electrons stored at the C–C bonds.

with PhN_3 and Me_3SiN_3 allowed the isolation of μ-phenylimido complexes **17** and **18**, derived from the oxidation of titanium(III) to titanium(IV), while the C–C bridging bond remained intact. These reactions provide evidence to support the hypothesis that, in the initial step, the incoming substrate binds and oxidizes the metal before drawing electrons from the C–C bond reservoir. Both compounds have been fully characterized. The low-quality X-ray structure of **17** and the proposed bond connectivity is reported in the data deposited at FIZ. In the case of **18**, controlled hydrolysis gave a complex which had retained the same skeleton, but in which the phenylimido group is replaced by a bridging oxo ligand in **19**, which has been structurally characterized (vide infra). A bridging bonding mode would be difficult in the case of hindered substituents at the azide functionality; thus the reaction probably follows a different pathway. Indeed, the reaction of **3** with Ph_3CN_3 resulted in the formation of the monomeric alkylimido **20** (Scheme 9).[18] The formation of **20** requires both the oxidation of the metal and a concomitant cleavage of the C–C bond. Its structure is discussed below. According to the distinctive tendency of vanadium to preferentially form terminal instead of bridging oxo or

0947-6539/99/0502-0714 $ 17.50+.50/0 *Chem. Eur. J.* **1999**, *5*, No. 2

phenylimido complexes, the latter type is a peculiarity of titanium, the reaction of **4** with PhN_3 led to the monomeric phenylimido complex **21** (Scheme 10).[19] This reaction parallels that of **4** with PyO which gives the corresponding oxovanadium(IV) complex **11** (Scheme 10).

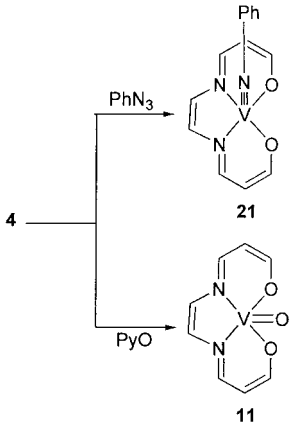

Scheme 10. Formation of vanadium(IV)-phenylimido and -oxo with electrons stored both at the C–C bond and at the metal.

The structure of **19** consists of two neutral dimeric $[\{Ti(salophen)\}_2(\mu\text{-}O)]$ units which both contain a C–C bond between two iminic carbon atoms of the adjacent salophen ligands (ligands A and B) [C(7)A – C(7)B, 1.587(10) Å]. The O(2) oxygen atom from the Schiff base B acts as a bridge between the metal atoms of adjacent dimeric units to produce the tetranuclear structure depicted in Figure 8. The tetramer

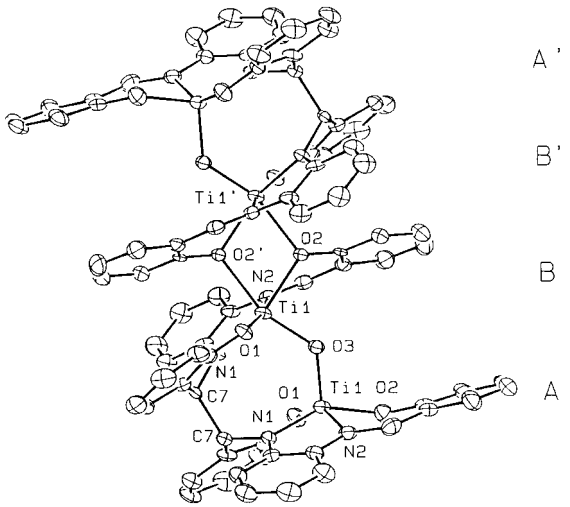

Figure 8. ORTEP view of complex **19** (30% probability ellipsoids). The prime denotes a transformation of $-x, 1-y, 1-z$.

possesses a crystallographically imposed C_i symmetry; the inversion center lies at the center of gravity of the Ti(1)-B,O(2)B,Ti(1)B′,O(2)B′ inner core. The coordination around Ti(1)A is square-pyramidal, with the base defined by the donor atoms of the salophen ligand A and the O(3) oxo oxygen atom at the apex. The N_2O_2 core is nearly planar, with deviations from planarity ranging from −0.012(6) to 0.012(6) Å for N(1)A and N(2)A, respectively. The Ti(1)A–O(3) vector forms a dihedral angle of 3.1(2)° with the normal to the N_2O_2 core. Hexacoordination around Ti(1)B is provided by the donor atoms of the salophen ligand B, namely the O(3) oxygen atom and the O(2)B′ oxygen atoms from the symmetry-related Schiff base. The metal atom is displaced by 0.195(2) Å out of the equatorial plane towards O(3). The Ti(1)A···Ti(1)B and Ti(1)B···Ti(1)B′ separations are 3.246(2) and 3.386(2) Å, respectively. The Ti–O(oxo) bond length is longer for the hexacoordinate [Ti(1)B–O(3), 1.847(5) Å] than for the pentacoordinate titanium [Ti(1)A–O(3), 1.787(4) Å]. The Ti–N bond lengths are shorter for the negatively charged N(1) atom [mean value 1.989(4) Å] than for the neutral N(2) atom [mean value 2.150(3) Å] (Table 2). As a consequence of the C–C bond formation, the six-membered chelation ring which involves the C(7) carbon atoms is folded along the C(7)···O(1) line; the dihedral angle between the Ti(1),N(1),C(7),O(1) and O(1),C(1),C(6),C(7) mean planes is 21.0(3) and 17.7(3)° for the salophen ligands A and B, respectively.

Complex **20** consists of discrete $[Ti(salophen)\{NC(Ph)_3\}]$ molecules (Figure 9). Titanium exhibits a square-pyramidal coordination with the N and O donor atoms from the salophen ligand at the base and the nitrogen atom from the

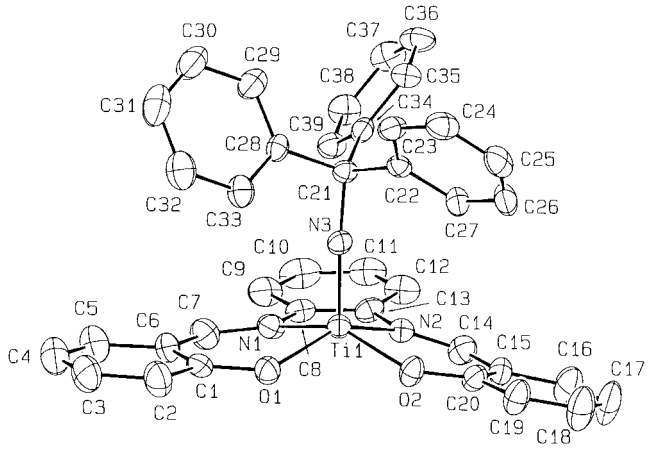

Figure 9. ORTEP view of complex **20** (30% probability ellipsoids).

imido ligand at the apex. The metal is displaced by 0.562(1) Å from the nearly planar N_2O_2 core (maximum displacements ranging from −0.014(4) to 0.014(4) Å). The line between Ti and N(3) forms a dihedral angle of 5.8(1)° with the normal to the N_2O_2 core. The Ti–N(3) bond length (1.686(4) Å) is in good agreement with the values reported in the literature for Ti–N(terminal nitrene) distances (e.g. 1.664(4) Å in dichloro(*tert*-butylimido)(*N*,*N*,*N*′,*N*′-tetramethylethylenediamine)titanium and 1.681(7) Å in dichloro(*tert*-butylimido)(*N*,*N*′-diisopropylethylenediamine)titanium.[20] The approximate linearity of the Ti-N(3)-C(21) bond angle (174.1(3)°) is in agreement with a Ti–N triple bond.

It should be emphasized that the reactions in Schemes 9 and 10 are a collection of two- and four-electron oxidations of the dimers **3** and **4**, and represent an interesting synthetic access to bridging and terminal metal–imido functionalities in macrocyclic chemistry.[21] In addition, these reactions provide

very interesting information on the occurrence of the redox reactions. It seems that the incoming reducible substrate binds the metal, and the interconnected processes, namely the oxidation of the metal, the formation of the metal–nitrogen double bond, and the cleavage of the carbon–carbon bond, occur as a cascade according to the sequence mentioned above. Therefore, the removal of electrons from the metal, then from the nitrogen will terminate with the cleavage of the C–C bond. This hypothesis is in agreement with the observation that not one of the oxidation reactions reported involves the C–C bond as a reactive site. We obtained significant support for such a hypothesis from the extended Hückel calculations carried out on the reduced species **6** and **7**.

Extended Hückel analysis on titanium and vanadium Schiff base complexes: Extended Hückel calculations[22, 23] were performed on the complexes [M(salophen)(Cl)(thf)] [M = Ti, V] and $[M_2(*salophen_2*)]^{2-}$, where *salophen$_2$* functions as a dinucleating, octadentate, octaanionic ligand (see Figure 4), in order to elucidate the nature of the reductive coupling of imino groups that leads to C–C bonded dimers. Such a reaction can be made reversible, so that the C–C bond functions as a unit to store and release electrons and which may be incorporated into rather complex structures. Our aim is to understand the role played by the transition metal in the redox process by means of an analysis of the electronic structure of the oxidized and the reduced species. The [M(salophen)(Cl)(thf)] complex was simplified by replacing thf with a water molecule, introduced in order to retain hexacoordination around the metal center. The oxidized form of the complexes has been investigated further by considering the M^{IV} complex [M(salophen)$(Cl)_2$] to be strictly related to the Zr^{IV} system [Zr(salophen)$(Cl)_2$(thf)],[3] as well as to the dimer $[\{M(salophen)(Cl)\}_2]$, in which the two units interact through oxygen bridges in a fashion similar to that found experimentally for $[\{Mn(salophen)(Py)\}_2]$.[2] For the reduced form of the complexes, we have considered only the species $[M_2(*salophen_2*)]^{2-}$, which is directly related to the experimental isolated system $[M_2(*salophen_2*)(Na)_2(thf)_6]$. The geometries, which were deduced from the available experimental X-ray structures, were idealized to C_{2v} symmetry for [M(salophen)$(Cl)_2$], C_s for [M(salophen)(Cl)(OH_2)], and C_i for the dimers $[\{M(salophen)(Cl)\}_2]$ and $[M_2(*salophen_2*)]^{2-}$.

Let us start our analysis with [Ti(salophen)Cl_2]. The molecular orbitals of this Ti^{IV} complex are reported in Figure 10. The lowest unoccupied molecular orbital (LUMO) is the $11b_1$ orbital, which is mainly C=N π-antibonding in character, with a strong polarization of the orbital towards the carbon centers. The reduction of this system should therefore imply a decrease of the carbon–nitrogen bond order and an acquisition of electron density, mainly by the carbon centers. This is confirmed by the Mulliken population analysis performed on the neutral and the reduced systems with a fixed geometry; these results are reported in Table 3 as net charges. The electron density increased by 0.12 e on Ti, 0.12 e on N, and 0.34 e on C for a one-electron reduction and by 0.23 e on Ti, 0.24 e on N, and 0.70 e on C for a two-electron reduction. A similar description applies also for [Ti(salophen)(Cl)(OH_2)] and $[\{Ti(salophen)(Cl)\}_2]$, although here the

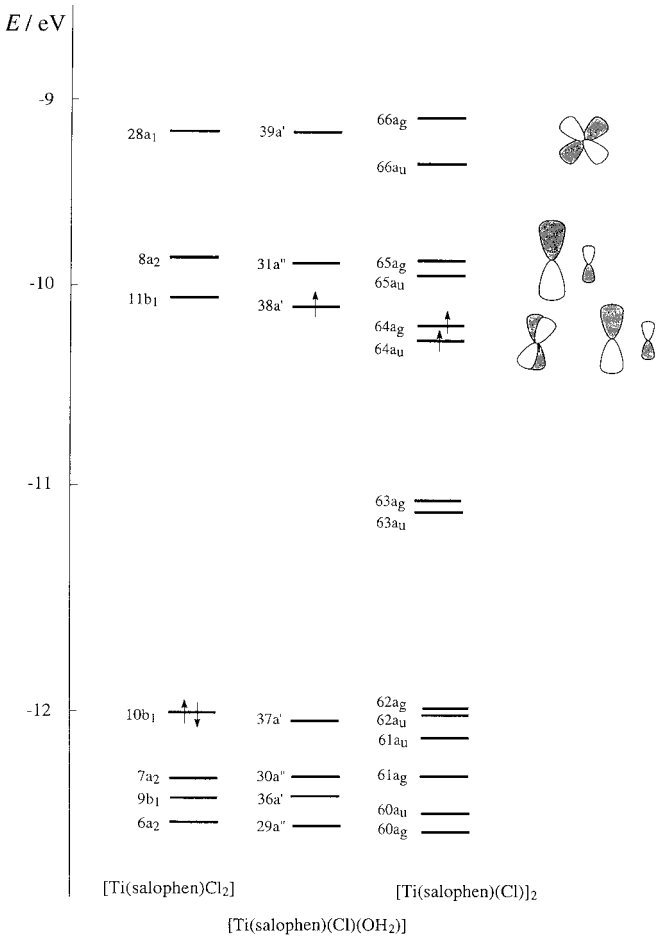

Figure 10. Energy levels of [Ti(salophen)Cl_2], [Ti(salophen)(Cl)(OH_2)], and $[\{Ti(salophen)(Cl)\}_2]$.

Table 3. Net charges (electronic units), obtained by Mulliken population analysis, on the centers involved in the redox process of the titanium complex.

	Charge of the system	Q(Ti)	Q(N)	Q(C)
[Ti(salophen)Cl_2]	0	1.64	−0.59	0.46
	−1	1.52	−0.65	0.29
	−2	1.41	−0.71	0.11
[Ti(salophen)(Cl)(OH_2)]	0	1.71	−0.63	0.31
	−1	1.46	−0.67	0.15
	−2	1.44	−0.72	−0.07
$[\{Ti(salophen)(Cl)\}_2]$	0	1.81	−0.64	0.29
	−2	1.56	−0.66	0.16
	−4	1.47	−0.70	0.01
$[Ti_2(*salophen_2*)]^{2-}$	−2	1.48	−0.70	0.24
	0	2.25	−0.63	0.25
	2	2.29	−0.47	0.27

picture is more complicated because of the presence of unpaired electrons. For [Ti(salophen)(Cl)(OH_2)] the 38a′ orbital is singly occupied. This orbital is mainly Ti d_{xz} and C=N π-antibonding in character, while the 31a″, which is the LUMO, is essentially C=N π-antibonding in character and is polarized towards the carbon center. For $[\{Ti(salophen)(Cl)\}_2]$ the $64a_u$ and $64a_g$ orbitals are singly occupied and show a character similar to the 38a′ orbital of [Ti(salophen)-(Cl)(OH_2)], while the $65a_u$ and $65a_g$ orbitals, which are

0947-6539/99/0502-0716 $ 17.50+.50/0 *Chem. Eur. J.* **1999**, *5*, No. 2

unoccupied, are essentially C=N π-antibonding in character. For these systems also, an increase in the electron density of the carbon centers upon reduction is observed, though we have an additional slight decrease in the oxidation state of the metal. Indeed, from Table 3 we can see that the electron density increases by 0.25 e on Ti, 0.08 e on N, and 0.32 e on C for a one-electron reduction and by 0.27 e on Ti, 0.18 e on N, and 0.76 e on C for a two-electron reduction for [Ti(salophen)(Cl)(OH_2)]. For the dimer [{Ti(salophen)(Cl)}$_2$] we have to consider a two- and a four-electron reduction: in Table 3 we notice that the overall increase in the electron density is 0.50 e on Ti (0.25 e for each metal center), 0.08 e on N, and 0.52 e on C for a two-electron reduction, and 0.68 e on Ti, 0.24 e on N, and 1.12 e on C for a four-electron reduction.

The molecular orbitals of [Ti_2(*salophen$_2$*)]$^{2-}$ are reported in Figure 11, which also includes the interactions with the

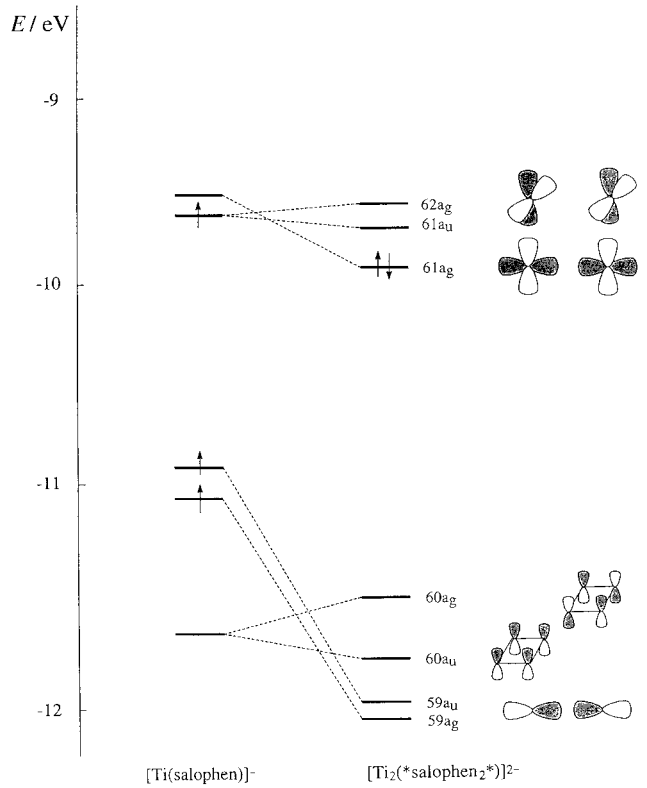

Figure 11. Molecular orbital diagram for the [Ti_2(*salophen$_2$*)]$^{2-}$ complex which depicts the interactions with the frontier orbitals of two [Ti(salophen)]$^-$ units.

frontier orbitals of two [Ti(salophen)]$^-$ units. The $59a_g$ and $59a_u$ orbitals describe the C–C σ bonds between the two salophen units, while the $60a_u$ and $60a_g$ are mainly composed of N p orbitals perpendicular to the N_4 plane. A small delocalization of these orbitals towards the rings coplanar to the N_4 core is present. The $61a_g$, which is the highest occupied molecular orbital (HOMO), is mainly Ti $d_{x^2-y^2}$ and binds the two titanium atoms. Small N p components are present, which also ascribe a weak Ti–N bonding character to this orbital. The lowest unoccupied orbitals, $61a_u$ and $62a_g$, are essentially titanium δ orbitals. Therefore, the oxidation of this system implies, as a first step, the oxidation of the metal centers and does not affect the C–C σ bonds between the two salophen units, at least as long as the geometry does not change, while a more pronounced oxidation strongly involves the nitrogen centers. This is confirmed by the Mulliken population analysis (Table 3): the electron density decreases overall by 1.54 e on Ti (0.77 e for each metal center), 0.28 e on N, and 0.04 e on C for a two-electron oxidation and by 1.62 e on Ti, 0.92 e on N, and 0.12 e on C for a four-electron oxidation.

A similar description also applies for the analogous vanadium complexes. In particular, as we can see from Figure 12, which presents the molecular orbital diagram for the [V_2(*salophen$_2$*)]$^{2-}$ complex, the orbitals describing the C–C σ bondings between the two salophen units, which are the $59a_g$ and $59a_u$ orbitals, are more than 2 eV lower than the energy of the HOMO in this system as well. The $60a_u$ and $60a_g$ orbitals are mainly N p perpendicular to the N_4 plane in character, while the $61a_g$ orbital describes the bonding between the two vanadium atoms. The $61a_u$ and $62a_g$ orbitals, which constitute the HOMO and the LUMO for the singlet state, are very close in energy to vanadium δ-orbitals. This situation gives rise to an excited triplet state very close to the singlet state, which is suggested to be the ground state from the experimental magnetic behavior of [V_2(*salophen$_2$*)-$(Na)_2(thf)_6$]. The oxidation of the [V_2(*salophen$_2$*)]$^{2-}$ system should therefore strongly affect the vanadium centers. This is confirmed by the Mulliken population analysis performed on [V_2(*salophen$_2$*)]$^{2-}$ and its oxidized species at fixed geometry. The electron density decreased by 0.91 e on each vanadium atom for the release of two electrons, and by 1.76 e for the release of four electrons, while the electron densities on N and C remain almost unchanged.

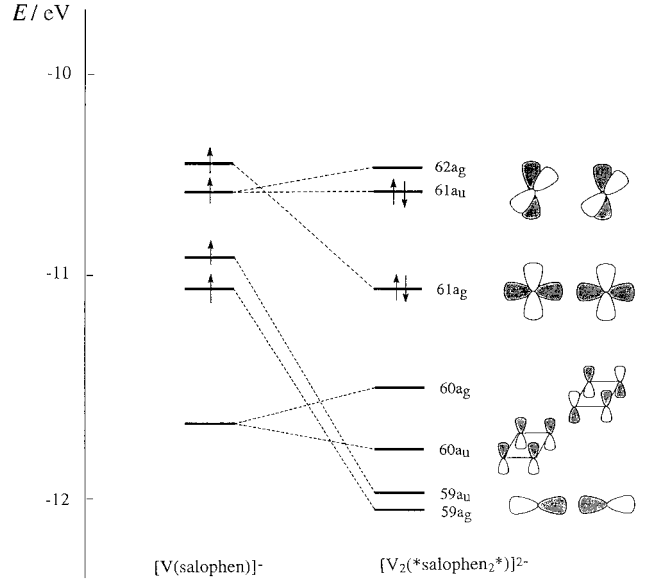

Figure 12. Molecular orbital diagram for the [V_2(*salophen$_2$*)]$^{2-}$ complex depicting the interactions with the frontier orbitals of two [V(salophen)]$^-$ units.

Conclusions

This report deals with a rather unique investigation into the chemical reduction of early transition metal–Schiff base complexes. This kind of experimental approach enabled us to

discover: i) the possibility of investigating the reduction pathways of π-delocalized ligands in the case of metals which are difficult to reduce; ii) a novel mode of storing and releasing electrons based on the reversible formation and cleavage of C–C bonds; iii) C–C bonds which function as two-electron reservoirs without being involved in the chemical reactivity; iv) the metal-assisted long-range electron transfer from the C–C bonds to incoming substrates; v) the introduction (see the nitrene reactivity) of important functionalities by the use of the electron-rich forms.

Experimental Section

General procedure: All reactions were carried out in an atmosphere of purified nitrogen. Solvents were dried and distilled before use by standard methods. Infrared spectra were recorded with a Perkin–Elmer FT1600 spectrophotometer, UV/Vis spectra were recorded with a Hewlett–Packard 8452A diode array spectrophotometer, and NMR spectra were recorded on a Bruker AC200 instrument. Phenyl azide was prepared according to the reported procedure.[24] Magnetic susceptibility was measured at 80–300 K on a MPMS5 SQUID susceptometer (Quantum Design) operating at a magnetic field strength of 3 kOe. Corrections were applied for diamagnetism calculated from Pascal constants.

Synthesis of Ph_3CN_3: NaN_3 (6 g, 100 mmol) was suspended in $CHCl_3$ (80 mL) in a three-necked flask equipped with a mechanical stirrer. The suspension was cooled to $-5\,^{\circ}C$ in an ice–salt bath, and then trifluoroacetic acid (28.6 g, 250 mmol) was added. After 10 min, triphenylmethanol (13 g, 50 mmol) was added to give a yellow slurry that slowly became white. This mixture was kept at $-5\,^{\circ}C$ for 3.5 h, and was then allowed to reach room temperature. The mixture was neutralized by the slow addition of an aqueous solution of ammonia (12%, 36 mL) and then transferred to a separation funnel. The organic layer was separated and the aqueous solution extracted with fresh $CHCl_3$ (80 mL). The combined organic extracts were then washed with water (50 mL), separated, dried over $MgSO_4$, and filtered. The solvent was removed under vacuum to give a pale yellow oil. Yield: 14.04 g (98%). As far as we found, this azide can be handled without any particular precautions. ^1H NMR (200 MHz, $CDCl_3$, 298 K): $\delta = 7.34$ (br s); IR (liquid film): $\tilde{\nu}_{max} = 2096$ (s), 1955 (w), 1810 (w), 1732 (w), 1594 (w), 1486 (m), 1445 (s), 1252 (m), 1210 (w), 1084 (w), 1032 (w), 943 (w), 898 (w), 760 (s), 715 (m), 696 (s), 667 (w), 626 (w) cm^{-1}.

Synthesis of 1·thf: Sodium hydride (7.0 g, 292 mmol) was slowly added to a yellow suspension of (salophen)H_2 (42.4 g, 134 mmol) in THF (1100 mL). This mixture was stirred at room temperature for 10 min, then refluxed for 1 h. The suspension was filtered and the yellow solid extracted with the mother liquor to remove excess sodium hydride. To the resulting orange solution was added $TiCl_3 \cdot 3$thf (49.6 g, 134 mmol) to give a deep blue suspension, which was then refluxed for 3 h. The product was filtered and the solid extracted with the mother liquor from the filtration, which was better than fresh solvent, in order to eliminate sodium chloride. The suspension was reduced to half of its volume and the deep blue product dried in a vacuum. Yield: 62 g (85%); IR (nujol): $\tilde{\nu}_{max} = 1597$ (s), 1567 (s), 1548 (w), 1525 (s), 1493 (m), 1430 (s), 1338 (m), 1321 (s), 1283 (m), 1257 (m), 1231 (m), 1192 (s), 1152 (s), 1126 (m), 1062 (s), 1030 (s), 967 (m), 927 (s), 878 (m), 818 (s), 788 (w), 755 (s), 664 (w), 625 (s), 601 (w), 587 (w), 558 (m), 541 (s), 511 (w), 486 (s), 459 (m), 441 (w) cm^{-1}; anal. calcd for $C_{28}H_{30}ClN_2O_4Ti$: C 62.06, H 5.58, N 5.17; found: C 61.89, H 5.27, N 5.28.

Synthesis of 2·thf:

Method A: Sodium hydride (4.19 g, 175 mmol) was slowly added to a yellow suspension of (salophen)H_2 (20.5 g, 64.8 mmol) in THF (500 mL) and the mixture stirred at room temperature for 10 min, then refluxed for 1 h. The suspension was filtered and the yellow solid extracted with the mother liquor in order to remove excess sodium hydride. To the resulting orange solution was added $VCl_3 \cdot 3$thf (23.2 g, 64.8 mmol) to give a brown suspension which was refluxed for 3 h. The product was extracted with the mother liquor to eliminate sodium chloride. The suspension was reduced to half of its volume and the brown product collected and dried in a vacuum. Yield: 28.3 g (80%); anal. calcd for $C_{28}H_{30}ClN_2O_4V$: C 61.71, H 5.55, N 5.14; found: C 61.07, H 5.35, N 4.88.

Method B: Tributylamine (18.8 g, 100 mmol) was added to a solution of (salophen)H_2 (12.84 g, 40.6 mmol) in THF (250 mL). The color turned from yellow to brown after the addition of $VCl_3 \cdot 3$thf (14.5 g, 40.6 mmol). The suspension was refluxed for 3 h and then allowed to stand at room temperature for 1 h. The crystalline brown product was filtered, washed with cooled THF (50 mL), and dried in a vacuum. Yield: 18.83 g (85%); IR (nujol): $\tilde{\nu}_{max} = 1602$ (s), 1574 (s), 1532 (s), 1318 (m), 1256 (m), 1191 (m), 1152 (m), 1032 (w), 924 (m), 868 (m), 814 (m), 758 (s), 622 (m), 538 (m), 497 (w) cm^{-1}; UV/Vis (THF): λ_{max} (ε_{max}, $M^{-1}cm^{-1}$) = 308 (20400), 336 (17500), 388 (14100), 435 sh nm (8000); anal. found: C 61.45, H 5.31, N 5.11.

Synthesis of 3·thf:

Method A: Sodium sand (386 mg, 16.8 mmol) was added to a dark blue suspension of **1**·thf (9.09 g, 16.8 mmol) in THF (250 mL). This mixture was stirred at room temperature for 3 days. Sodium chloride was filtered off and the solvent was evaporated to dryness. The brown residue was then treated with Et_2O (150 mL) to give a suspension from which a brown microcrystalline product was collected. Yield: 5.69 g (78%); anal. calcd for $C_{48}H_{44}N_4O_6Ti_2$: C 66.37, H 5.10, N 6.45; found: C 66.18, H 5.11, N 6.45.

Method B: **1**·thf (3.54 g, 6.53 mmol) was added to a brown solution of **6** (3.93 g, 3.27 mmol) in THF (500 mL). This mixture was stirred at room temperature for 4 days. Sodium chloride was filtered off and the solvent was evaporated to dryness. The residue was then treated with pentane (150 mL), to give a suspension from which a brown product was collected and dried in a vacuum. Yield: 4.9 g (86%); IR (nujol): $\tilde{\nu}_{max} = 1593$ (m), 1544 (w), 1270 (s), 1190 (w), 1106 (m), 1081 (m), 1026 (m), 907 (m), 863 (m), 808 (w), 753 (s), 639 (m), 553 (w) cm^{-1}; anal. found: C 66.51, H 5.42, N 6.73.

Synthesis of 4:

Method A: Sodium sand (133 mg, 5.80 mmol) was added to a brown suspension **2**·thf (3.16 g, 5.80 mmol) in THF (250 mL). This mixture was stirred at room temperature for 3 days. Sodium chloride was filtered off and the solvent was evaporated to dryness. The brown residue was then treated with Et_2O (100 mL) resulting in a suspension from which a dark violet microcrystalline product was collected and dried in a vacuum. Yield: 2.1 g (83%); anal. calcd for $C_{48}H_{44}N_4O_6V_2$: C 65.91, H 5.07, N 6.41; found: C 65.10, H 5.40, N 6.89.

Method B: **2**·thf (6.22 g, 11.4 mmol) was added to a brown solution of **7** (6.90 g, 5.71 mmol) in THF (500 mL). This mixture was stirred at room temperature for 2 days. Sodium chloride was filtered off and the solvent was evaporated to dryness. The brown residue was then treated with Et_2O (200 mL) to give a suspension from which a dark violet microcrystalline product was collected and dried in a vacuum. Yield: 3.5 g (70%); IR (nujol): $\tilde{\nu}_{max} = 1600$ (s), 1578 (m), 1528 (m), 1267 (m), 1144 (w), 1028 (w), 917 (w), 856 (w), 750 (s), 606 (w), 544 (m), 438 (w) cm^{-1}; UV/Vis (THF): λ_{max} (ε_{max}, $M^{-1}cm^{-1}$) = 294 sh (33400), 392 (16600), 548 nm (5920); anal. found: C 64.99, H 5.77, N 6.18. Recrystallization from THF/Py produced crystals of [Ti_2(salophen$_2$)(Py_2)] (**5**) which were suitable for X-ray analysis.

Synthesis of 6:

Method A: Sodium sand (0.418 g, 18.2 mmol) was added to a dark blue suspension of **1**·thf (4.68 g, 8.64 mmol) in THF (250 mL). The color immediately turned dark green and then slowly brown-red. The suspension was stirred at room temperature for 30 min, then refluxed for 2 h. Sodium chloride was filtered off and the solution was concentrated to 30 mL. Et_2O (70 mL) was added dropwise and the suspension was left to stand overnight at room temperature. A brown crystalline product was collected and dried in a vacuum. Yield: 3.92 g (75%); anal. calcd for $C_{64}H_{76}N_4Na_2O_{10}Ti_2$: C 63.89, H 6.37, N 4.66; found: C 63.23, H 5.71, N 4.84.

Method B: Sodium sand (0.280 g, 12 mmol) was added to a brown suspension of **3** (5.21 g, 6 mmol) in THF (300 mL). The mixture was stirred for 2 days. The solution was concentrated to 30 mL before Et_2O (100 mL) was added dropwise. The suspension was left to stand overnight at room temperature and the brown crystalline product was collected and dried in a vacuum. Yield: 5.56 g (77%); IR (nujol): $\tilde{\nu}_{max} = 1586$ (w), 1546 (w), 1255 (s), 1147 (w), 1103 (w), 1045 (s), 895 (w), 845 (w), 753 (m), 730 (s), 639 (w) cm^{-1}; anal. found: C 63.38, H 5.98, N 4.36;

Synthesis of 7:

Method A: Sodium sand (0.214 g, 9.33 mmol) was added to a brown suspension of **2**·thf (2.31 g, 4.24 mmol) in THF (100 mL). This mixture was

0947-6539/99/0502-0718 $ 17.50+.50/0 *Chem. Eur. J.* **1999**, *5*, No. 2

stirred at room temperature overnight and then refluxed for 3 h. Sodium chloride was filtered off, the brown solution was reduced to half of its volume, Et_2O (100 mL) was added, and the solution was then left at 0 °C for 12 h. An amber microcrystalline solid was collected and dried in a vacuum. Yield: 1.81 g(71 %); anal. calcd for $C_{64}H_{76}N_4Na_2O_{10}V_2$: C 63.57, H 6.33, N 4.63; found: C 63.16, H 6.91, N 4.95.

Method B: Sodium sand (184 mg, 8 mmol) was added to a brown suspension of **4** (3.5 g, 4 mmol) in THF (150 mL) and the mixture was stirred for 2 days. The solvent was evaporated to dryness and the residue was treated with Et_2O (100 mL), collected, and dried it in a vacuum. Yield: 1.76 g (73 %); IR (nujol): $\tilde{\nu}_{max} = 1589$ (m), 1561 (w), 1282 (s), 1233 (m), 1105 (w), 1085 (w), 1049 (s), 801 (w), 756 (s), 726 (s), 706 (m), 542 (w) cm^{-1}; UV/Vis (THF): λ_{max} (ε_{max}, $M^{-1}cm^{-1}$) = 286 (39400), 340 sh nm (21000); anal. found: C 62.96, H 6.33, N 4.12.

Reaction of 3 with $PhCH_2Cl$: Freshly distilled benzyl chloride (4.39 g, 34.7 mmol) was added to a solution of **3** (1.46 g, 1.68 mmol) in THF (125 mL), the mixture was refluxed overnight, and allowed to cool to room temperature. A brown microcrystalline solid precipitated. The solvent was evaporated to dryness and [Ti(salophen)Cl_2] was then stirred in Et_2O (100 mL), filtered, and dried in a vacuum. Yield: 1.16 g (80 %); ^1H NMR (200 MHz, [D_6]acetone, 298 K): $\delta = 7.98$ (s, 1H, CH), 7.02 (m, 2H, Ar), 6.91 (m, 2H, Ar), 6.63 (m, 2H, Ar); IR (nujol): $\tilde{\nu}_{max} = 1594$ (s), 1572 (s), 1544 (s), 1294 (m), 1267 (s), 1235 (m), 1200 (m), 1150 (w), 1117 (w), 1033 (w), 967 (w), 922 (m), 867 (m), 833 (s), 750 (s), 661 (s), 567 (w), 540 (m), 485 (m), 440 (w) cm^{-1}; anal. calcd for $C_{20}H_{14}N_2O_2Cl_2Ti$: C 55.46, H 3.26, N 6.49; found: C 55.81, H 3.73, N 6.28.

Reaction of 4 with $PhCH_2Cl$: Freshly distilled benzyl chloride (3.24 g, 25.6 mmol) was added to a solution of **4** (1.25 g, 1.43 mmol) in THF (100 mL). The mixture was refluxed overnight and allowed to cool to room temperature. A brown microcrystalline solid precipitated. The solution was concentrated to 2/3 of its initial volume, **2**·thf was collected and dried in a vacuum. Yield: 1.36 g (87 %); anal. found: C 61.83, H 5.28, N 5.07. For spectroscopic data vide supra.

Reaction of 4 with $[(Cp)_2Fe]^+[BPh_4]^-$, synthesis of 8: To a solution of **4** (1.17 g, 1.34 mmol) in THF (150 mL) at −40 °C was added $[(Cp)_2Fe]^+[BPh_4]^-$ (2.17 g, 4.29 mmol) in one portion. The mixture was allowed to slowly reach room temperature and a color change from violet to dark-orange was observed. The solvent was evaporated to dryness and the brown residue was suspended in hexane (150 mL). The orange solution was discarded and the brown solid extracted in hot THF (100 mL). The solvent was evaporated to dryness and the product was suspended in hexane (100 mL), collected, and dried in a vacuum. Yield: 2 g (89 %); IR (nujol): $\tilde{\nu}_{max} = 1945$ (w), 1883 (w), 1821 (w), 1603 (s), 1533 (s), 1439 (s), 1304 (m), 1282 (w), 1264 (w), 1238 (w), 1191 (w), 1151 (m), 1122 (w), 1104 (w), 1031 (w), 1016 (w), 965 (w), 922 (w), 864 (m), 813 (m), 754 (m), 729 (m), 700 (s), 627 (m), 609 (m), 540 (m), 496 (w), 442 (w) cm^{-1}; anal. calcd for $C_{52}H_{50}BN_2O_4V$: C 75.72, H 5.99, N 3.33; found: C 75.33, H 6.18, N 3.04

Synthesis of 9: Complex **3** (2.80 g, 3.22 mmol) was added to a solution of 9,10-phenanthrenequinone (1.34 g, 6.45 mmol) in THF (250 mL). The brown suspension was refluxed overnight and then concentrated to half of its volume. Hexane (100 mL) was added, and the brown solid was then filtered and dried in a vacuum. Yield: 3.10 g (75 %); ^1H NMR (200 MHz, [D_6]DMSO, 298 K): $\delta = 9.53$ (s, 1H, CH=N); 8.49 (dd, $J_o = 6.8$ Hz, $J_m =$ 2.0 Hz, 1H, quin); 8.05 (m, 1H, Ar); 7.91 (dd, $J_o = 6.8$ Hz, $J_m = 2.0$ Hz, 1H, quin); 7.75 (td, $J_o = 6.8$ Hz, $J_m = 2.0$ Hz, 1H, quin); 7.55 (m, 1H, Ar); 7.26 (m, 1H, Ar); 7.16 (t, $J = 6.8$ Hz, 1H, quin); 7.04 (m, 2H, Ar); 6.85 (m, 1H, Ar); 3.58 (m, 2H, THF); 1.75 (m, 2H, THF); IR (nujol): $\tilde{\nu}_{max} = 1608$ (s), 1580 (s), 1543 (s), 1489 (m), 1441 (s), 1334 (w), 1294 (s), 1281 (s), 1200 (w), 1150 (m), 1123 (w), 1110 (w), 1059 (m), 1026 (m), 925 (w), 861 (m), 814 (m), 790 (w), 754 (s), 724 (w), 690 (w), 640 (s), 623 (m), 600 (s), 543 (m), 486 (m), 452 (w), 412 (m) cm^{-1}; anal. calcd for $C_{38}H_{30}N_2O_5Ti$: C 71.03, H 4.71, N 4.36; found: C 70.29, H 4.63, N 4.28.

Synthesis of 10: Complex **4** (1.9 g, 2.17 mmol) was added to a solution of 9,10-phenanthrenequinone (0.9 g, 4.34 mmol) in THF (150 mL). The brown suspension was refluxed overnight and was then concentrated to half of its volume. Hexane (100 mL) was added and the brown solid was filtered and dried in a vacuum. Yield: 1 g (71 %); μ_{eff} (293 K) = 1.61 BM; IR (nujol): $\tilde{\nu}_{max} = 1606$ (s), 1572 (s), 1533 (s), 1439 (s), 1311 (s), 1256 (w), 1194 (m), 1150 (s), 1028 (m), 922 (w), 850 (w), 806 (m), 750 (s), 722 (m), 622 (w), 539 (m), 500 (w) cm^{-1}; anal. calcd for $C_{38}H_{30}N_2O_5V$: C 70.70, H 4.68, N 4.34; found: C 70.78, H 4.73, N 4.14.

Reaction of 4 with *p*-benzoquinone, synthesis of 11: Complex **4** (1.37 g, 1.57 mmol) was added to an orange solution of *p*-benzoquinone (0.169 g, 1.57 mmol) in THF (100 mL). The resulting dark green suspension was stirred for 20 min and then refluxed overnight. The solvent was evaporated to dryness and the residue was treated with hexane (100 mL), collected, and dried in a vacuum. Yield of **11**·thf: 1.15 g (80 %); IR (nujol): $\tilde{\nu}_{max} = 1600$ (s), 1578 (m), 1528 (m), 1267 (m), 1144 (w), 1028 (w), 917 (w), 856 (w), 750 (s), 606 (w), 544 (m), 438 (w) cm^{-1}; anal. calcd for $C_{24}H_{22}N_2O_4V$: C 63.58, H 4.89, N 6.18; found: C 63.13, H 4.20, N 6.03.

Reaction of 3 with dioxygen, synthesis of 14: A solution of **3** (0.92 g, 1.06 mmol) in THF (100 mL) was exposed to dry oxygen. The color changed from brown to dark red and a pale brown solid precipitated. Gas volumetry showed that the solution absorbed 1.02 mmol of O_2 within 160 min. The solid was collected and dried in a vacuum. Yield: 0.71 g (88 %); IR (nujol): $\tilde{\nu}_{max} = 1612$ (s), 1583 (s), 1539 (s), 1444 (s), 1311 (s), 1189 (m), 1140 (m), 1117 (w), 1033 (w), 922 (w), 872 (m), 817 (m), 750 (s), 623 (m), 540 (m), 490 (w), 450 (w) cm^{-1}; anal. calcd for $C_{20}H_{14}N_2O_3Ti$: C 63.51, H 3.73, N 7.41; found: C 62.71, H 3.98, N 6.73.

Reaction of 4 with dioxygen: A solution of **4** (1.18 g, 1.35 mmol) in THF (100 mL) was exposed to dry oxygen. The color changed from violet to dark green. Gas volumetry showed that the solution absorbed 1.04 mmol of O_2 within 129 min. The solvent was evaporated to dryness and was washed with hexane (100 mL), the green product was collected and dried in a vacuum. Yield of **11**·thf: 1 g (81 %); anal. found: C 63.73, H 4.21, N 6.85. For spectroscopic data vide supra.

Reaction of 7 with dioxygen: A solution of **7** (1.33 g, 1.1 mmol) in THF (100 mL) was exposed to dry oxygen. An immediate color change from brown to wine-red was observed. Gas volumetry showed that the solution absorbed 2.3 mmol of O_2. The solvent was evaporated to dryness and the pale brown residue was suspended in doubly distilled water. The product was obtained by filtration of the Na_2O_2-containing solution and recrystallization from $CHCl_3$. Yield of complex **11**: 0.5 g (60 %); anal. calcd for **11**, $C_{20}H_{14}N_2O_3V$: C 63.00, H 3.70, N 7.35; found: C 63.26, H 3.58, N 7.67. For spectroscopic data vide supra.

Synthesis of 16: Complex **7** (2.3 g, 1.90 mmol) was dissolved in DME (110 mL). The brown solution was exposed to a slow diffusion of O_2 for 8 h, until the color turned deep violet. The mixture was then allowed to stand at −5 °C for 3 days. The crystalline solid which formed was collected and analyzed. Yield: 220 mg (13 %); IR (nujol): $\tilde{\nu}_{max} = 1606$ (s), 1585 (s), 1536 (m), 1481 (s), 1440 (s), 1322 (s), 1270 (s), 1172 (w), 1151 (m), 1128 (w), 1050 (m), 949 (s), 920 (m), 865 (w), 801 (w), 746 (s), 732 (s), 627 (m), 610 (m), 569 (w), 543 (m), 506 (w), 474 (w), 431 (w) cm^{-1}; anal. calcd for **16**, $C_{44}H_{44}N_4Na_2O_{10}V_2$: C 65.00, H 5.45, N 6.32; found: C 64.73, H 5.11, N 6.88).

Synthesis of 17: Phenyl azide (0.442 g, 3.71 mmol) was added to a solution of **3** (1.61 g, 1.85 mmol) in THF (90 mL). The color immediately turned dark red. The mixture was stirred overnight and then concentrated to 30 mL. *n*-Hexane (100 mL) was added dropwise and the product was collected and dried in a vacuum. Yield: 1.35 g (76 %). Crystals suitable for X-ray analysis were grown in a toluene solution. ^1H NMR (200 MHz, CD_3CN, 298 K): $\delta = 9.18$ (s, 2H, CH=N); 7.95 (m, 2H, Ar); 7.71 (dd, $J_o =$ 7.8 Hz, $J_m = 1.5$ Hz, 2H, Ar); 7.55–7.45 (m, 4H, Ar); 7.09–6.81 (m, 13H, Ar); 6.71–6.36 (m, 8H, Ar); 5.85 (s, 2H, CH-N); 3.65 (m, 8H, THF); 1.8 (m, 8H, THF); IR (nujol): $\tilde{\nu}_{max} = 1600$ (s), 1578 (s), 1533 (s), 1444 (s), 1306 (s), 1272 (s), 1144 (m), 1028 (w), 922 (w), 856 (m), 750 (s), 622 (m), 544 (w) cm^{-1}; anal. calcd for **17**, $C_{54}H_{49}N_5O_6Ti_2$: C 67.58, H 5.15, N 7.30; found: C 67.18, H 5.05, N 7.03.

Synthesis of 18: Trimethylsilyl azide (0.53 g, 4.60 mmol) was added to a suspension of **3** (2 g, 2.30 mmol) in THF (100 mL). The mixture was stirred overnight, refluxed for 30 min, and then filtered and dried. The product was washed with *n*-hexane (100 mL), collected, and dried in a vacuum. Yield: 1.17 g (63 %); ^1H NMR (200 MHz, C_6D_6, 298 K): $\delta = 8.36$ (s, 2H, CH=N), 7.40–6.10 (m, 24H, Ar), 5.71 (s, 2H, CH=N), −0.19 (s, 9H, CH_3); IR (nujol): $\tilde{\nu}_{max} = 1596$ (s), 1575 (s), 1440 s), 1307 (m), 1280 (m), 1030 (w), 920 (w), 856 (w), 750 (s), 620 (m), 545 (w) cm^{-1}; anal. calcd for **18**, $C_{43}H_{37}N_5O_4SiTi$: C 63.63, H 4.59, N 8.63; found: C 63.08, H 4.51, N 8.57.

Synthesis of 19: Complex **18** (0.4 g, 0.493 mmol) was dissolved in wet toluene (70 mL). The solution was stirred for 1 day and then allowed to stand at −2 °C for 2 days. A red-brown solid was collected and dried in a

vacuum. Yield: 0.036 g (9.92%). Crystals suitable for X-ray analysis were grown in the mother liquor. ^{1}H NMR (200 MHz, C_6D_6, 298 K): $\delta = 8.23$ (s, 2H, CH=N), 7.52–5.98 (m, 24H, Ar), 5.68 (s, 2H, CH-N); anal. calcd for **19**, $C_{40}H_{28}N_4O_5Ti_2$: C 64.89, H 3.81, N 7.57; found: C 64.21, H 3.98, N 7.95.

Synthesis of 20: Complex **3** (2.10 g, 2.42 mmol) was added to a solution of triphenylmethyl azide (1.38 g, 4.83 mmol) in THF (150 mL). The solution was stirred for 6 h, refluxed for 1 h, then allowed to reach room temperature, and left to stand overnight which gave a precipitate. The solution was concentrated to 20 mL and *n*-hexane (100 mL) was added dropwise. The brown product was collected and dried in a vacuum. Yield: 2.03 g (67.8%). Crystals suitable for X-ray analysis were grown in a THF/Et_2O solution. ^{1}H NMR (200 MHz, TDF, 298 K): $\delta = 8.99$ (s, 2H, CH=N), 7.83 (dd, 2H, $J_o = 6.35$ Hz, $J_m = 2.93$ Hz, Ar salophen); 7.55–7.40 (m, 6H, Ar salophen), 7.37 (dd, 2H, $J_o = 6.35$ Hz, $J_m = 2.93$ Hz, Ar salophen), 7.08 (d, 2H, $J = 8.30$ Hz, Ar salophen), 6.90–6.65 (m, 17H, Ar salophen + Ph); IR (nujol): $\tilde{\nu}_{max} = 1601$ (s), 1576 (s), 1534 (s), 1440 (s), 1315 (s), 1221 (s), 1191 (s), 1145 (s), 1121 (m), 1076 (w), 1024 (w), 963 (w), 921 (w), 888 (w), 864 (w), 846 (w), 815 (m), 788 (w), 754 (s), 697 (s), 636 (m), 621 (m), 557 (w), 542 (s), 496 (m), 481 (w), 460 (w), 442 (w), 416 (m) cm^{-1}; anal. calcd for **20**, $C_{39}H_{29}N_3O_2Ti$: C 75.61, H 4.72, N 6.78; found: C 75.34, H 4.81, N 6.93.

Reaction of 4 with PhN_3, synthesis of 21: Phenyl azide (0.332 g, 2.79 mmol) was added to a solution of **4** (1.22 g, 1.39 mmol) in THF (100 mL). An immediate color change from violet to brown was observed. The mixture was stirred overnight and a microcrystalline solid separated. The solution was concentrated to 40 mL and hexane (100 mL) was then added dropwise. Then the product collected and dried in a vacuum. Yield: 1.18 g (80%); μ_{eff} (295 K) = 1.77 BM; IR (nujol): $\tilde{\nu}_{max} = 1605$ (s), 1578 (s), 1534 (s), 1434 (s), 1315 (s), 1257 (w), 1233 (w), 1187 (s), 1150 (s), 1126 (w), 1066 (w), 1029 (w), 996 (w), 969 (w), 923 (m), 899 (w), 859 (w), 809 (m), 788 (w), 752 (s), 685 (m), 621 (m), 604 (m), 558 (m), 541 (s), 501 (m), 481 (m), 447 (w), 404 (m) cm^{-1}; anal. calcd for **21**, $C_{30}H_{27}N_3O_3V$: C 68.18, H 5.15, N 7.95; found: C 68.17, H 4.68, N 8.72.

Reaction of 4 with pyridine-*N*-oxide: Pyridine-*N*-oxide (0.131 g, 1.38 mmol) was added to a violet solution of **4** (1.01 g, 1.15 mmol) in THF (100 mL). The mixture was refluxed overnight to give a dark green solution. The solvent was evaporated to dryness and the residue treated with hexane (100 mL). The product was collected and dried in a vacuum. Yield: of **11**·thf: 0.9 g (85%); anal. found: C 63.35, H 4.34, N 6.37. For spectroscopic data vide supra.

X-ray crystallography for complexes 5–7, 16, 19, and **20**: Suitable crystals were mounted in glass capillaries and sealed under nitrogen. The reduced cells were obtained with the use of TRACER.[25] Data for complexes **5–7**, **16**, and **19** were collected on a single-crystal diffractometer (Philips PW1100 for **5**, **7**, and Rigaku AFC6S for **6**, **16**, **19**) at 295 K for **5**, **7**, **19** and 138 K for **6**, **16**. Data for complex **20** were collected on a KUMA CCD at 295 K. For intensities and background, individual reflection profiles were analyzed.[26] The structure amplitudes were obtained after the usual Lorentz and polarization corrections[27] and the absolute scale was established by the Wilson method.[28] The crystal quality was tested by ψ-scans which showed that crystal absorption effects could be neglected except for **6**, **16**, and **19**. Data of complexes **6**, **16**, and **19** were then corrected for absorption by a semiempirical method.[29] Anomalous scattering corrections were included in all structure factor calculations.[30b] Scattering factors for neutral atoms were taken from ref. [30a] for non-hydrogen atoms and from ref. [31] for H.

Structure solutions were based on the observed reflections $[I > 2\sigma(I)]$. The structures were solved by the heavy-atom method starting from a three-dimensional Patterson map.[32] The least-square refinements were carried out using the unique reflections with $F^2 > 0$ by minimizing the function $\Sigma w(\Delta F^2)^2$.[33] The weighting scheme $w = 1/[\sigma^2(F_o)^2 + (aP)^2]$ $(P = (F_o^2 + 2F_c^2)/3)$, based on the counting statistics, was applied. In the last refinement cycles *a* converged at 0.0585, 0.1430, 0.0820, 0.0728, 0.0571, and 0.0352 for **5**, **6**, **7**, **16**, **19**, and **20** respectively. Refinement was performed with full-matrix least-squares, first isotropically, then anisotropically for all the non-H atoms except for the disordered atoms. The hydrogen atoms, but not those associated with the disordered carbon atoms, which were ignored, were located from difference Fourier maps and introduced in the subsequent refinements as fixed contributions with isotropic U's fixed at 0.08 Å^2 for **5**, **7**, and **20** and 0.05 Å^2 for **6**, **16**, and **19**.

The final difference maps showed no peaks which had a chemical meaning above the general background, except for a peak of 1.02 e Å^{-3} in **6** located midway along the Ti(1)–N(2) bond.

The refinement of complexes **16** and **20** was straightforward.

Complex ***5***: The three THF solvent molecules of crystallization were affected by severe disorder. The O(3), C(32)–C(34) and O(4), C(35)–C(38) THF molecules were found to be statistically distributed over two positions about an inversion center and a two-fold axis, respectively. The atoms were therefore isotropically refined with a site occupation factor of 0.5. The O(5), C(39)–C(42) THF molecule was distributed over four positions about a two-fold axis. The best fit was obtained by splitting the O(5) atom over two positions (A and B) and isotropically refining the atoms with a site occupation factor of 0.75 for C(40), C(42) and 0.25 for O(5)A, O(5)B, C(39), and C(41). During the refinement, the C–O and C–C bond lengths within the disordered THF solvent molecules were constrained to be 1.48(1) and 1.54(1) Å, respectively.

Complex ***6***: The C(31) carbon atom of a coordinated THF molecule showed high thermal parameters which indicate the presence of disorder. The atom was then split over two positions (A and B) and isotropically refined with site occupation factors of 0.8 and 0.2, respectively. One THF molecule was found to be statistically distributed over two positions about an inversion center approximately sharing the C(33) atom and alternatively coordinating the sodium cations of adjacent complexes. The best fit was obtained by isotropically refining the O(6), C(34), and C(35) atoms with a site occupation factor of 0.5 and anisotropically refining the C(33) atom. The C(41)–C(44) carbon atoms of the THF solvent molecule of crystallization were found to be disordered over two positions (A and B) and were isotropically refined with a site occupation factor of 0.5. During the refinement, the C–O and C–C bond lengths involving the disordered THF solvent molecules were constrained to be 1.48(1) and 1.54(1) Å, respectively.

Complex ***7***: The C(22), C(27), and C(28) carbon atoms of THF molecules coordinated to the sodium cation showed high thermal parameters which indicate the presence of disorder. The best fit was found by splitting the atoms over two positions (A and B) and were isotropically refined with a site occupation factor of 0.5. Additionally, ten independent residual peaks were interpreted in terms of one THF solvent molecule of crystallization disordered over two positions and isotropically refined with a site occupation factor of 0.5. The position of the oxygen atom could not be unambiguously determined.

Complex ***19***: The C(21)–C(27) toluene solvent molecule of crystallization was found to be statistically distributed over two positions (C and D) and was isotropically refined with site occupation factors of 0.5. The disordered aromatic rings were constrained to have a D_{6h} symmetry.

Complex ***20***: Since the complex crystallizes in a polar space group, the crystal chirality was tested by inverting the coordinates $(x,y,z \rightarrow x,-y,-z)$ and refining to convergence again. The resulting *R* values quoted in brackets in Table 1 indicated that the original choice should be considered to be the correct one.

Further details of the crystal structure investigations may be obtained from the Fachinformationszentrum Karlsruhe, D-76344 Eggenstein-Leopoldshafen (Germany) (fax: (+49) 7247-808-606; e-mail: crysdata@fiz.karlsruhe.de) on quoting the depository numbers CSD-410113 (**5**), 410114 (**6**), 410115 (**7**), 410116 (**16**), 410117 (**17**), 410118 (**19**), 410119 (**20**).

Acknowledgments

We thank the Fonds National Suisse de la Recherche Scientifique (Bern, Switzerland, Grant No. 20-53′336.98) and Ciba Specialty Chemicals (Basel, Switzerland) for financial support. Some earlier exploratory work by M. Mazzanti is acknowledged.

[1] B. Dietrich, P. Viout, J.-M. Lehn, *Macrocyclic Chemistry*, VCH, Weinheim, **1993**; L. F. Lindoy, *The Chemistry of Macrocyclic Ligand Complexes*, Cambridge University Press, Cambridge, **1989**.

[2] E. Gallo, E. Solari, N. Re, C. Floriani, A. Chiesi-Villa, C. Rizzoli, *J. Am. Chem. Soc.* **1997**, *119*, 5144–5154.

  0947-6539/99/0502-0720 $ 17.50+.50/0 *Chem. Eur. J.* **1999**, *5*, No. 2

[3] E. Solari, C. Maltese, F. Franceschi, C. Floriani, A. Chiesi-Villa, C. Rizzoli, *J. Chem. Soc. Dalton Trans.* **1997**, 2903–2910.
[4] S. De Angelis, E. Solari, E. Gallo, C. Floriani, A. Chiesi-Villa, C. Rizzoli, *Inorg. Chem.* **1996**, *35*, 5995–6003.
[5] S. Gambarotta, C. Floriani, A. Chiesi-Villa, C. Guastini, *J. Chem. Soc. Chem. Commun.* **1982**, 756–758; S. Gambarotta, F. Urso, C. Floriani, A. Chiesi-Villa, C. Guastini, *Inorg. Chem*. **1983**, *22*, 3966–3972.
[6] S. Gambarotta, M. Mazzanti, C. Floriani, M. Zehnder, *J. Chem. Soc. Chem. Commun.* **1984**, 1116–1118.
[7] M. Pasquali, F. Marchetti, A. Landi, C. Floriani, *J. Chem. Soc. Dalton Trans.*, **1978**, 545–549.
[8] M. Mazzanti, S. Gambarotta, C. Floriani, A. Chiesi-Villa, C. Guastini, *Inorg. Chem.* **1986**, *25*, 2308–2314.
[9] F. A. Cotton, R. A. Walton, *Multiple Bonds Between Metal Atoms*, Clarendon, Oxford, **1993**.
[10] O. Kahn, *Molecular Magnetism*, VCH, New York, **1982**.
[11] a) P. Guerriero, S. Tamburini, P. A. Vigato, *Coord. Chem. Rev.* **1995**, *139*, 17–243; b) C. Floriani, F. Calderazzo, L. Randaccio, *J. Chem. Soc. Chem. Commun.* **1973**, 384–385; c) S. Gambarotta, F. Corazza, C. Floriani, M. Zehnder, *J. Chem. Soc. Chem. Commun.* **1984**, 1305–1307; d) C. P. Horwitz, Y. Ciringh, *Inorg. Chim. Acta* **1994**, *225*, 191–200; e) N. Bresciani-Pahor, M. Calligaris, P. Delise, G. Nardin, L. Randaccio, E. Zotti, G. Fachinetti, C. Floriani, *J. Chem. Soc. Dalton Trans* **1976**, 2310–2316; f) C. P. Horwitz, J. T. Warden, S. T. Weintraub, *Inorg. Chim. Acta* **1996**, *246*, 311–320; g) A. Giacomelli, C. Floriani, G. Perego, *J. Chem. Soc. Chem. Commun.* **1982**, 650–652; h) E. Solari, C. Floriani, D. Cunningham, T. Higgins, P. McArdle, *J. Chem. Soc. Dalton Trans.* **1991**, 3139–3143; i) B. R. Gibney, H. Wang, J. W. Kampf, V. L. Pecoraro, *Inorg. Chem.* **1996**, *35*, 6184–6193.
[12] The same kind of compound with a different counteranion has been structurally characterized in ref. [19].
[13] W. A. Nugent, J. M. Mayer, *Metal–Ligand Multiple Bond*, Wiley, New York, **1988**.
[14] F. Franceschi, E. Gallo, E. Solari, C. Floriani, A. Chiesi-Villa, C. Rizzoli, N. Re, A. Sgamellotti, *Chem. Eur. J.* **1996**, *2*, 1466–1476.
[15] a) N. P. Dwyer, L. Puppe, J. W. Buchler, W. R. Scheidt, *Inorg. Chem.* **1975**, *14*, 1782–1785; b) R. Guilard, J. M. Latour, C. Lecomte, J. C. Marchon, J. Protas, D. Ripoll, *Inorg. Chem.* **1978**, *17*, 1228–1237; c) R. Guilard, C. Lecomte, *Coord. Chem. Rev.* **1985**, *65*, 87; d) C. H. Yang, V. L. Goedken, *Inorg. Chim. Acta* **1986**, *117*, L19–L21; e) C. H. Yang, J. A. Ladd, V. L. Goedken, *J. Coord. Chem.* **1988**, *19*, 235–251; f) L. Peng-Ju, H. Sheng-Hua, H. Kun-Yao, T. C. W. Mak, *Inorg. Chim. Acta* **1990**, *175*, 105–110; g) G. E. Housmekerides, D. L. Ramage, C. M. Kretz, J. T. Shontz, R. S. Pilato, *Inorg. Chem.* **1992**, *31*, 4453–4468; h) M. R. Smith, III, P. T. Matsunaga, R. A. Andersen, *J. Am. Chem. Soc.* **1993**, *115*, 7049–7050; i) P. Jeske, G. Haselhorst, T. Weyhermueller, K. Wieghardt, B. Nuber, *Inorg. Chem.* **1994**, *33*, 2462–2471; j) D. J. Schwartz, M. R. Smith, III, R. A. Andersen, *Organometallics* **1996**, *15*, 1446–1450.
[16] a) E. Gallo, E. Solari, F. Franceschi, C. Floriani, A. Chiesi-Villa, C. Rizzoli, *Inorg. Chem.* **1995**, *34*, 2495–2496; b) S. De Angelis, E. Solari, C. Floriani, A. Chiesi-Villa, C. Rizzoli, *Organometallics* **1995**, *14*, 4505–4512; c) R. Crescenzi, E. Solari, C. Floriani, A. Chiesi-Villa, C. Rizzoli, *Organometallics* **1996**, *15*, 5456–5458.
[17] a) F. A. Cotton, S. A. Duraj, W. J. Roth, *Inorg. Chem.* **1984**, *23*, 4042–4045; b) S. L. Castro, Z. Sun, J. C. Bollinger, D. N. Hendrickson, G. Christou, *J. Chem. Soc. Chem. Commun.* **1995**, 2517–2518; c) M. R. Bond, R. S. Czernuszewicz, B. C. Dave, Q. Yan, M. Mohan, R. Verastegue, C. J. Carrano, *Inorg. Chem.* **1995**, *34*, 5857–5869.
[18] P. Mountford, *Chem. Commun.* **1997**, 2127–2134.
[19] a) D. D. Devore, J. D. Lichtenham, F. Takusagawa, E. A. Maatta, *J. Am. Chem. Soc.* **1987**, *109*, 7408–7416; b) J. de With, A. D. Horton, A. G. Orpen, *Organometallics* **1990**, *9*, 2207–2209; c) J. de With, A. D. Horton, A. G. Orpen, *Organometallics* **1993**, *12*, 1493–1496; d) J. de With, A. D. Horton, *Angew. Chem.* **1993**, *105*, 958–960; *Angew. Chem. Int. Ed. Engl.* **1993**, *32*, 903–905; e) H. Schumann, *Inorg. Chem.* **1996**, *35*, 1808–1813.
[20] T. S. Lewkebandara, P. H. Sheridan, M. J. Heeg, A. L. Rheingold, C. H. Winter, *Inorg.Chem*. **1994**, *33*, 5879–5889.
[21] P. Mountford, *Chem. Soc. Rev.* **1998**, *27*, 105–115.
[22] R. Hoffmann, W. N. Lipscomb, *J. Chem. Phys.* **1962**, *36*, 2179–2189.
[23] R. Hoffmann, *J. Chem. Phys.* **1963**, *39*, 1397–1412.
[24] R. O. Lindsay, C. F. H. Allen, *Organic Synthesis Collective, Vol. 3*, p. 711.
[25] S. L. Lawton, R. A. Jacobson, *TRACER (a cell reduction program)*, Ames Laboratory, Iowa State University of Science and Technology, Ames, IA, **1965**.
[26] M. S. Lehmann, F. K. Larsen, *Acta Crystallogr. Sect. A: Cryst. Phys. Diffr. Theor. Gen. Crystallogr*. **1974**, *30*, 580–584.
[27] Data reduction, structure solution, and refinement were carried out on a Quansan personal computer equipped with an INTEL Pentium processor, and on an ENCORE 91 computer.
[28] A. J. C. Wilson, *Nature* **1942**, *150*, 151.
[29] A. C. T. North, D. C. Phillips, F. S. Mathews, *Acta Crystallogr. Sect. A: Cryst. Phys. Diffr. Theor. Gen. Crystallogr.* **1968**, *24*, 351.
[30] a) *International Tables for X-Ray Crystallography*, *Vol. IV*, Kynoch, Birmingham, **1974**, p. 99; b) see ref. [30a], p. 149.
[31] R. F. Stewart, E. R. Davidson, W. T. Simpson, *J. Chem. Phys.* **1965**, *42*, 3175–3187.
[32] G. M. Sheldrick, SHELX 76, Program for Crystal Structure Determination, University of Cambridge, **1976**.
[33] G. M. Sheldrick, SHELXL 92, University of Göttingen, **1992**.

Received: June 5, 1998 [F1193]